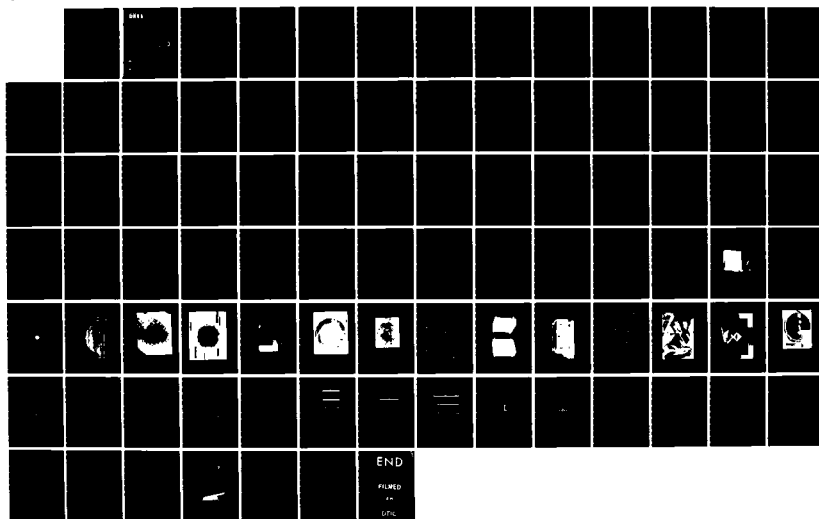
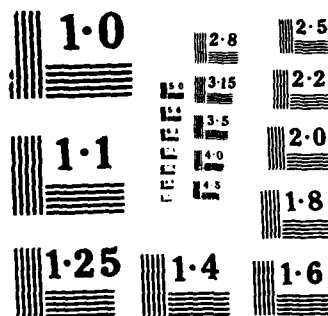


AD-A163 398

THE EFFECT OF AIR GAPS ON THE PROPAGATION OF DETONATION 1/1
IN CHARGES CONSIS. (U) DEFENCE RESEARCH ESTABLISHMENT
SUFFIELD RALSTON (ALBERTA) A W GIBB DEC 85 DRES-385
F/G 19/1 NL

UNCLASSIFIED





NATIONAL BUREAU OF STANDARDS
MICROCOPY RESOLUTION TEST CHART



National Défense
Defence nationale

UNCLASSIFIED

DRES

SUFFIELD REPORT

NO. 385

AD-A163 398

(2)

**THE EFFECT OF AIR GAPS ON THE PROPAGATION
OF DETONATION IN CHARGES CONSISTING OF
STACKED BLOCKS OF CAST TNT (U)**

by

A.W. Gibb

DTIC
ELECTE
JAN 28 1986
S D

DISTRIBUTION STATEMENT A

Approved for public release;
Distribution Unlimited

Project No. 27C20

DTIC FILE COPY

December 1985



DEFENCE RESEARCH ESTABLISHMENT SUFFIELD, RALSTON, ALBERTA

WARNING

The use of this information is permitted subject to
recognition of proprietary and patent rights

Canada

80 1 27 10 3

UNCLASSIFIED

DEFENCE RESEARCH ESTABLISHMENT SUFFIELD
RALSTON, ALBERTA

SUFFIELD REPORT NO. 385

THE EFFECT OF AIR GAPS ON THE PROPAGATION OF DETONATION
IN CHARGES CONSISTING OF STACKED BLOCKS OF CAST TNT (U)

by

A. W. Gibb

Project No. 27C20

WARNING

The use of this information is permitted subject to recognition
of proprietary and patent rights.

UNCLASSIFIED

UNCLASSIFIED

(i)

DEFENCE RESEARCH ESTABLISHMENT SUFFIELD
RALSTON, ALBERTA

SUFFIELD REPORT NO. 385

THE EFFECT OF AIR GAPS ON THE PROPAGATION OF DETONATION
IN CHARGES CONSISTING OF STACKED BLOCKS OF CAST TNT (U)

by

A. W. Gibb

ABSTRACT

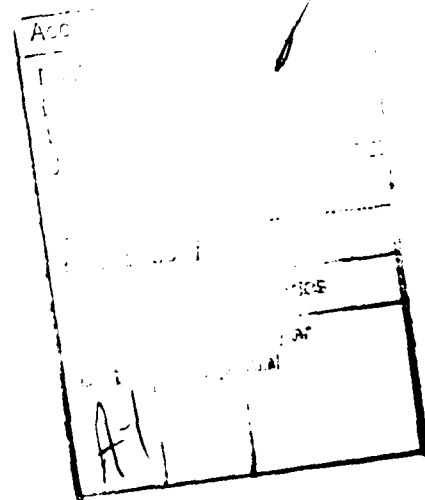
Results are reported for a series of experiments, the objective of which was to study the influence of air gaps on the propagation of detonation between large blocks of slow-cooled cast TNT. The blocks were prepared so as to be identical to blocks used in the construction of stacked 500 ton TNT charges for large-scale air blast experiments. A clear-pour technique was used, resulting in an ordered coarse crystal structure in the blocks. The experimental donor-receptor configurations were chosen to simulate two cases encountered on the interior of the large charges - a two-block configuration in which the detonation front was parallel to the block edge, and a four-block configuration in which the detonation front intersected the common corner between the blocks obliquely (at an angle of 45°). These effects were studied as a function of air gap width and confinement. In the two-block experiments, detonation propagated successfully across air gaps up to 75 mm. Detonation wave shape was unaffected when the front was parallel to the edge of the gap. Measured detonation velocity was 5% lower, and results in the receptor blocks more scattered, when the propagation vector was parallel to the long axis of the TNT crystals. In the four-block

UNCLASSIFIED

UNCLASSIFIED

(ii)

experiments, air gaps up to 25 mm were studied. Luminous detonation products were observed to channel ahead of the detonation front in the air gaps adjacent to the donor block. In the diagonally-opposite receptor block, the channelled detonation product gases played a rôle in the re-initiation of detonation by initiating two low-velocity reaction waves along the block edges, from the point of intersection of which a stable detonation front emerged travelling approximately parallel to the original front in the donor block. The new detonation front was, however, delayed with respect to the front in the donor block. The delay increased as the air gap width was increased and decreased when the blocks were confined by plexiglass.



UNCLASSIFIED

ACKNOWLEDGEMENTS

The author wishes to acknowledge the substantial contribution of M.A. Nolan and J.B. Dempsey to the organization and conduct of approximately thirty experiments which contributed to this report. Mr. Nolan also played a key rôle in the commissioning of the field laboratory and instrumentation systems used in this work. Thanks are also due to Pamela Alink and Valerie Hill for their diligent and careful work in digitizing the film records. Cooperation of staff members of Field Operations Section, particularly members of the Hazardous Materiel Group and Field Trials Officers R. Withers and P. Mast, in casting, preparation, set-up and firing of the TNT blocks is gratefully acknowledged. Finally, the author extends his thanks to responsible managers J.S. Watson, J.H.B. Anderson and R.T. Schmitke of the Military Engineering Section, DRES, for their support of this work.

TABLE OF CONTENTS

ABSTRACT.....	i
ACKNOWLEDGEMENTS.....	iii
TABLE OF CONTENTS.....	iv
LIST OF TABLES.....	vi
LIST OF FIGURES.....	vii
NOMENCLATURE.....	ix
1.0 INTRODUCTION.....	1.
2.0 BACKGROUND.....	2.
2.1 DESCRIPTION OF TNT CHARGES.....	2.
2.2 TYPES OF ANOMALIES.....	3.
2.3 POSSIBLE SOURCES OF ANOMALIES.....	3.
2.3.1 GENERAL.....	3.
2.3.2 VARIABLE CRYSTAL STRUCTURE.....	4.
2.3.3 INHOMOGENEITIES WITHIN THE BLOCKS.....	5.
2.3.4 PHYSICAL OR CHEMICAL IMPURITIES.....	6.
2.3.5 DISCONTINUITIES (AIR GAPS) BETWEEN THE BLOCKS.....	7.
2.3.6 TAYLOR INSTABILITY.....	7.
2.3.7 INFLUENCE OF AIR GAPS ON FORMATION OF ANOMALIES.....	8.
3.0 DESCRIPTION OF EXPERIMENTS.....	9.
3.1 EXPERIMENTAL PLAN.....	9.
3.1.1 CHOICE OF EXPERIMENTAL GEOMETRIES.....	9.
3.1.2 CHOICE OF GAP SIZE.....	10.
3.1.3 CHOICE OF CONFINEMENT MEDIUM.....	11.
4.0 EXPERIMENTAL TECHNIQUE.....	11.
4.1 GENERAL.....	11.
4.2 CHARGE PREPARATION PROCEDURE.....	12.
4.2.1 CASTING OF TNT BLOCKS.....	12.

TABLE OF CONTENTS

4.2.2	CASTING OF RESISTIVE DETONATION VELOCITY PROBES INTO TNT BLOCKS.....	12.
4.2.3	CUTTING OF TNT BLOCKS.....	12.
4.2.4	PREPARATION OF EXPERIMENTAL CHARGE.....	13.
4.3	INSTRUMENTATION.....	14.
4.3.1	ULTRA-HIGH SPEED PHOTOGRAPHY.....	14.
4.3.2	CONTINUOUS RESISTIVE DETONATION VELOCITY PROBES.....	15.
5.0	DATA ANALYSIS TECHNIQUES	15.
5.1	FRAMING RECORD.....	15.
5.2	STREAK RECORD.....	16.
5.3	RESISTIVE DETONATION VELOCITY PROBE.....	16.
5.4	ESTIMATION OF ERROR.....	17.
6.0	DISCUSSION OF RESULTS.....	17.
6.1	CONFIGURATION 1 (TWO TNT BLOCKS).....	18.
6.2	CONFIGURATION 2 (TWO TNT BLOCKS).....	19.
6.3	CONFIGURATION 3 (FOUR TNT BLOCKS).....	20.
6.4	RESULTS OF OTHER WORKERS.....	24.
6.4.1	TWO-BLOCK CONFIGURATIONS (PARALLEL INCIDENCE).....	24.
6.4.2	EFFECT OF CRYSTAL ORIENTATION.....	25.
6.4.3	FOUR-BLOCK CONFIGURATION (OBLIQUE INCIDENCE).....	27.
6.4.3.1	Internal Channel Effect.....	27.
6.4.3.2	Relation to Present Work.....	29.
7.0	CONCLUSIONS AND RECOMMENDATIONS.....	29.
8.0	REFERENCES.....	31.

TABLES

FIGURES

ANNEX A - DESCRIPTION OF CASTING PROCEDURE FOR TNT BLOCKS

ANNEX B - EXPLOSIVE PLANE-WAVE GENERATOR

ANNEX C - RESISTIVE DETONATION VELOCITY PROBE SYSTEM

UNCLASSIFIED

(vi)

LIST OF TABLES

- TABLE 1 - SUMMARY OF RESULTS FROM CONFIGURATION 1 EXPERIMENTS
- TABLE 2 - SUMMARY OF RESULTS FROM CONFIGURATION 2 EXPERIMENTS
- TABLE 3 - SUMMARY OF RESULTS FROM CONFIGURATION 3 EXPERIMENTS
- TABLE 4 - DETONATION VELOCITIES FROM HOLSGROVE REPORT

UNCLASSIFIED

LIST OF FIGURESFigure
No.

1. CAST TNT BLOCK USED IN CONSTRUCTION OF LARGE-SCALE TNT CHARGES AT DRES
2. SIDE VIEW, CENTRE SECTION THROUGH 100 TON TNT CHARGE
3. TOP VIEW, CENTRE SECTION THROUGH 100 TON TNT CHARGE
4. SIDE VIEW OF STACKED 500 TON TNT HEMISPHERE TANGENT TO GROUND SURFACE
5. TOP VIEW OF LARGE-SCALE TNT CHARGE, PARTLY CONSTRUCTED, SHOWING ALTERNATE LAYERS ROTATED BY 45°
6. AERIAL VIEW OF DETONATING 500 TON TNT CHARGE SHOWING ALL TYPES OF ANOMALIES
7. CROSS-SECTION THROUGH CENTRE OF TNT BLOCK REVEALING CRYSTAL STRUCTURE
8. AERIAL PHOTOGRAPH OF LAYER 13 FROM 500 TON CHARGE (PRAIRIE FLAT)
9. EARLY TIME PHOTOGRAPH FROM SPHERICAL 20 TON BLOCK-BUILT TNT CHARGE SHOWING NON-UNIFORM LIGHT BREAKOUT AT CHARGE SURFACE
10. BLOCK CONFIGURATIONS USED IN EXPERIMENTS
11. PHOTOGRAPH OF TNT MOLD
12. PHOTOGRAPH OF MOLD WITH BOTTOM REMOVED SHOWING DETONATION VELOCITY PROBES SUSPENDED IN MOLD READY FOR CASTING
13. PORTIONS OF TNT BLOCKS FROM CONFIGURATIONS 1 - 3 USED IN EXPERIMENTS
14. CUTTING OF TNT BLOCK USING STEAM KNIFE
15. PHOTOGRAPH OF FOUR-BLOCK EXPERIMENT (CONFIGURATION 3) READY FOR FIRING
16. CORDIN MODEL 330A CAMERA
17. PLAN VIEW OF EXPERIMENTAL LAYOUT SHOWING MIRROR ARRANGEMENT FOR CAMERA OPTICS
18. PORTIONS OF RESISTIVE PROBES IN TNT BLOCKS
19. COMPOSITE DRAWING FROM FRAMING RECORD
20. TYPICAL DIGITIZED RECORD FROM STREAK FILM
21. TYPICAL DIGITIZED RECORDS FROM RESISTIVE DETONATION VELOCITY PROBES
22. DETONATION VELOCITY MEASUREMENTS FROM CONFIGURATION 1 EXPERIMENTS (UNCONFINED BLOCKS)

LIST OF FIGURES (cont'd)Figure
No.

23. DETONATION VELOCITY MEASUREMENTS FROM CONFIGURATION 1 EXPERIMENTS (CONFINED BLOCKS)
24. DETONATION VELOCITY MEASUREMENTS FROM CONFIGURATION 2 EXPERIMENTS (UNCONFINED BLOCKS)
25. COMPOSITE TRACINGS FROM FRAMING CAMERA SHOWING PROGRESS OF DETONATION FRONT ACROSS AIR GAPS (UNCONFINED TNT BLOCKS)
26. COMPOSITE TRACINGS FROM FRAMING CAMERA SHOWING LINES OF CONSTANT PROPAGATION VELOCITY (UNCONFINED TNT BLOCKS)
27. CHANGES IN SHAPE AND POSITION OF DETONATION FRONT IN RECEPTOR BLOCKS CAUSED BY 3 MM AIR GAP
28. CHANGES IN SHAPE AND POSITION OF DETONATION FRONT IN RECEPTOR BLOCKS CAUSED BY 13 MM AIR GAP
29. CHANGES IN SHAPE AND POSITION OF DETONATION FRONT IN RECEPTOR BLOCKS CAUSED BY 25 MM AIR GAP
30. HOLSGROVE'S EXPERIMENTAL CONFIGURATION (HOLSGROVE, 1968)
31. EFFECT OF AIR GAP WIDTH ON DETONATION VELOCITY IN RECEPTOR BLOCK (HOLSGROVE, 1968)
32. MODEL FOR CHANNEL EFFECT
33. DETONATION VELOCITIES IN CYLINDERS OF HIGH EXPLOSIVES 21 MM IN DIAMETER AFTER AHRENS (1965)
34. MOUSETRAP-TYPE PLANE WAVE GENERATOR

UNCLASSIFIED

(ix)

NOMENCLATURE

ρ_0	initial gas density before passage of shock front
ρ_1	density of gas immediately after passage of shock front
w	shock front velocity
u	particle velocity of compressed gas
D	propagation velocity of detonation front
D_t	axial detonation propagation velocity for tubular solid explosive charges
D_c	largest detonation velocity that is possible in steady-state detonation (for a density corresponding to the crystal density)
ΔV	voltage change across resistive detonation velocity probe at any instant of time
i_0	constant current passing through resistive probe
dR/dx	resistance per unit length of resistive probe
x	distance along resistive probe, measured from crimped end of probe

UNCLASSIFIED

UNCLASSIFIED

DEFENCE RESEARCH ESTABLISHMENT SUFFIELD
RALSTON, ALBERTA

SUFFIELD REPORT NO. 385

THE EFFECT OF AIR GAPS ON THE PROPAGATION OF DETONATION
IN CHARGES CONSISTING OF STACKED BLOCKS OF CAST TNT (U)

by

A. W. Gibb

1.0 INTRODUCTION

From 1958-1970, a series of large-scale blast trials was conducted on the range of the Defence Research Establishment Suffield (DRES). The purpose of these trials, conducted under the auspices of Panel N2 of The Technical Co-operation Program (TTCP), was to simulate the air blast effects from detonation of a 1 kton nuclear weapon at ground level. Military targets were arrayed at carefully chosen distances from the charge. The charges consisted of 500 Tons of cast TNT in the form of approximately 30,000 TNT blocks stacked in a careful geometrical arrangement to produce the desired overall shape (either a sphere tangent to the ground surface or a hemisphere). Each charge was centrally initiated.

On all of the shots in this series, anomalous behaviour of the fireball and shock wave was observed when the charge was detonated. An irregular fireball with large protuberances and jet-like fingers extending a great distance from ground-zero was documented by both ground level and aerial cameras. The fireball irregularities and shock-wave protuberances were termed anomalies. These anomalies produced air blast loadings that were unpredictable in both magnitude

UNCLASSIFIED

and direction and usually compromised the results at target locations in their path. Considerable attention was devoted between 1964 and 1970 to understanding and eliminating the cause of these anomalies, culminating in a TTCP Panel N2 Technical Summary Report¹ published in 1970. This report identified five distinct types of anomalies and discussed several possible causes of the anomalies. In more recent large-scale blast trials, stacks of bagged ammonium nitrate/fuel oil (AN/FO) have replaced the stacked TNT blocks, since AN/FO is less expensive and seems to generate fewer anomalies.

The purpose of the experiments described in the present report was to investigate one of the propositions discussed in Reference 1, namely, that air gaps between blocks of TNT in the large block-built TNT charges might be a contributing cause of the observed anomalies. Section 2 presents background information concerning types of anomalies observed on the large block-built TNT charges and discusses possible causes of the anomalies. Section 3 contains a description of the experimental configurations chosen to highlight the influence of air gaps on detonation propagation, while Section 4 explains the experimental techniques employed. Section 5 describes methods used to analyze data from the ultra-high-speed camera and electronic probes. Section 6 discusses experimental results and compares the results with those of other workers. Finally, Section 7 presents conclusions which can be drawn from the results presented in this report and discusses implications for the large block-built TNT charges.

2.0 BACKGROUND

2.1 DESCRIPTION OF TNT CHARGES

The basic charge of interest in this report was a cast TNT block (Figure 1) weighing approximately 15 kg (33 lb). The block had dimensions 30.5 cm x 30.5 cm x 10.2 cm. The blocks were prepared for the present experiments using exactly the same methods employed at DRES to prepare blocks for the large-scale blast trials. The exact casting procedure is described in Annex A.

Details of a typical stacking arrangement used in the large-scale blast trials are shown in Figures 2, 3, 4 and 5. Successive horizontal layers were rotated 45° with respect to each other.

2.2 TYPES OF ANOMALIES

As mentioned in the Introduction, Reference 1 identified five distinct types of anomalies. All five are shown in Figure 6. This figure is an aerial photograph of DISTANT PLAIN Event 6 (100-ton block-built spherical charge tangent to and above the ground). The following text is quoted from Reference 1:

"1. Five types of anomalies have been identified:

TYPE 1 - Luminous precursor jets from the fireball which move ahead of the main shock.

TYPE 2 - Non-luminous precursor jets from the fireball which move ahead of the main shock.

TYPE 3 - Non-luminous surface precursor jets containing surface material.

TYPE 4 - Shock perturbations which apparently do not contain solid material.

TYPE 5 - Fireball perturbations which affect the shock front."

The anomalies of greatest interest are Types 1, 2, 4 and 5. The type 3 anomaly is apparently caused by an air shock wave/ground interaction and is not of interest in the present report.

2.3 POSSIBLE SOURCES OF ANOMALIES

2.3.1 GENERAL

Before describing the mechanisms advanced as possible causes of blast anomalies, it is worthwhile to review briefly observations of the anomalies described above. The following text is reproduced from Reference 1:

"Jetting and perturbations of the shock front profile have been observed on small as well as large charges, cast and pressed charges as well as block-built charges, rectangular and hemispherical as well as spherical charges, Pentolite and PETN as well as TNT, and free-air as well as surface-burst charges. Indeed, the anomalies observed appear to be due to the nature of explosions emanating from solid explosives.

"In contrast to the anomalies observed on solid charge explosions, no anomalies have been observed on detonable gas, liquid charge explosions, or bagged or bulk AN/FO contained in cardboard shells. Anomalies have been observed on 20- and 100- ton AN/FO charges contained in fiberglass shells. Admittedly, few observations have been made on these types of charges. However, the little evidence in hand on their behaviour and the observations of the gross characteristics of the anomalies from the solid charges offer a clue to the probable root cause for the anomalies observed, namely, the intrinsic mechanical structure of the charges or their containers. Solid charges, prepared by casting, have a definite crystalline structure; solid charges prepared by pressing and prilled ammonium nitrate-fuel oil have a granular structure; and, of course, liquid and gaseous charges are fluid with no grain or crystal structure. Block-built charges have a structure characteristic of the stacking arrangement."

Reference 1 lists and discusses several possible causes of anomalies. These are:

- (i) variable crystal structure within the blocks
- (ii) inhomogeneities within the blocks
- (iii) physical or chemical impurities within the blocks
- (iv) discontinuities (air gaps) between the blocks.

2.3.2 VARIABLE CRYSTAL STRUCTURE

Variations in crystal structure within the blocks occur because the blocks are produced by solidification in molds of a crystalline material (TNT). The size and orientation of crystals at a specific point in the material are

influenced by the rate of cooling and the solidification pattern established for the block as a whole. These are in turn influenced by such factors as the surface-to-volume ratio, thermal conductivity of the mold and cooling medium with which the mold is in contact, and shape of the mold. All of the TNT blocks produced at DRES for the large-scale blast trials were produced using standardized aluminum molds and solidification procedures.² An example of the influence of the casting process on the final crystal structure in the blocks is provided by the following quotations from Reference 1:

"The 12- x 12- x 4-inch blocks used on the post-1960 Canadian trials and on the SAILOR HAT tests were similar; both were made of reclaimed TNT and both were cast in the same way and at the same temperature. There was one basic difference, however, in the preparation of the blocks. The Canadian blocks were cooled after pouring in a cold water bath until solid. The SAILOR HAT blocks were cooled in a cold water bath for only forty-five minutes; solidification of the charge took place at room temperature in about 5 to 6 hours. These slightly different cooling procedures resulted in large shaped crystals across the 4-inch width of the Canadian blocks with plane cleavage faces. The SAILOR HAT blocks had somewhat smaller crystals with some interlacing of crystal structure and irregular cleavage faces. It was observed that the Canadian blocks were more fragile than the SAILOR HAT blocks; they tended to break along the crystal boundaries."

A centre section through a TNT block cast at DRES is shown in Figure 7. The crystal structure can be clearly seen.

2.3.3 INHOMOGENEITIES WITHIN THE BLOCKS

Inhomogeneities observed within the blocks include air voids, irregular crystal patterns, hairline cracks, and gradations in colour which could correspond to density variations.

Air voids and hairline cracks generally occur as a consequence of the substantial shrinkage which occurs in TNT upon solidification. A large air void forces the detonation front to pass around it, causing a local distortion of the

shape of the front. It is well-known³ that small air voids can result in increased explosive sensitivity, as a shock wave impacting the near edge of the void collapses the void to produce a local temperature well in excess of the temperature achieved through shock compression of the solid material. Hairline cracks may lead to cleavage of the block during or after it is placed in position in the stack, making a portion of the block susceptible to partial or incomplete detonation and to ejection from the stack, particularly if it is located at or near the charge surface.

Irregular crystal patterns, and gradations in colour reflecting possible density variations, may be caused by lack of uniformity in the cooling pattern. The influence of irregular crystal patterns is discussed in Section 2.3.2. The detonation velocity in cast solid explosive is known to be a linear function of initial density.⁴ Local variations in density, if present, will lead to a corresponding local variation in detonation velocity.

2.3.4 PHYSICAL OR CHEMICAL IMPURITIES

The presence of physical or chemical impurities in the blocks used on the large-scale blast trials is a consequence of the fact that, on most shots, the TNT was supplied from a combination of U.S., British and Canadian sources, and most of it was reclaimed TNT, far from military specification purity. One evidence of the presence of impurities can be seen in Figure 8 which shows an aerial photograph of layer 13 from the 500 ton charge used in Operation Prairie Flat. The British TNT has a much darker colour than the lighter-coloured U.S. and Canadian blocks. Furthermore, while the U.S. and Canadian TNT blocks were randomly distributed throughout the layers, in this particular charge the British TNT was concentrated in two layers. If the impurities in these particular blocks adversely affected the progress of the detonation front, anomalous detonation propagation could have resulted.

2.3.5 DISCONTINUITIES (AIR GAPS) BETWEEN THE BLOCKS

The following quotation from Reference 1 is pertinent:

"Block-built charges may be even more conducive to producing jets than solid charges. In addition to the inhomogeneities present in most cast blocks, the block construction introduces discontinuities between blocks. Holsgrove⁵ in preliminary work shows the sudden drop in detonation velocity as the detonation wave propagates from one TNT block into the abutting block. He also indicates that it takes about 4 inches of travel through the acceptor block before the full detonation velocity is reached. Wisotski⁶ in his experiments with a single row of stacked pressed TNT blocks shows discontinuities in the explosive product envelope as each interface between blocks is reached. In short, experimental evidence indicates that a discontinuity can have an adverse effect on the detonation potential of any small volume of charge.

"It is to be noted that, in the normal stacking of large charges with 12- x 12- x 4-inch blocks, only the blocks in the equatorial plane have their 12-inch dimension lined up with the direction of propagation of the detonation front. Most other blocks are shorter in terms of radial detonation front propagation path. The blocks in the vertical plane have only 4 inches of charge through which to obtain full detonation velocity. In the light of Holsgrove's work (also reported by others), 4 inches of charge length is barely sufficient to attain full detonation velocity for TNT."

2.3.6 TAYLOR INSTABILITY

The term Taylor instability refers to a phenomenon first identified by Sir Geoffrey Taylor.⁷ Consider two adjacent fluids of different densities accelerated in a direction perpendicular to their interface. Taylor showed that the uniform interface is unstable when the acceleration is directed from the lighter to the heavier fluid. This would be the case for a spherically-expanding (decelerating) shock wave and fireball in air. The occurrence of one or more

Taylor instabilities during the decelerative expansion of shock wave and fireball in air could explain at least some of the anomalies (shock perturbations, luminous and non-luminous precursor jets). The theory of Taylor instabilities makes two significant predictions:

(i) that these instabilities can occur even when the fluids involved have initially very uniform properties. Thus, anomalies attributable to Taylor instabilities would be observed on very uniform charges such as small cast or pressed solid spheres and gaseous mixtures contained in spherical gas bags. This prediction is consistent with experimental observation.

(ii) rate of development of a Taylor instability is reduced as the ratio of densities in the two fluids tends towards unity. This prediction can explain why substantially fewer large anomalies have been observed in stacked Ammonium Nitrate/Fuel Oil (AN/FO) charges than in stacked TNT charges, and virtually no anomalies have been observed in detonations of large spherical gas bags. The bulk density of AN/FO is substantially smaller than the density of TNT, while the density of gaseous mixtures is much closer to that of air than either of the above.

2.3.7 INFLUENCE OF AIR GAPS ON FORMATION OF ANOMALIES

A striking high-speed photograph (Figure 9, reproduced from Reference 1) of a spherical 20 ton block-built TNT charge detonated on a tower, illustrates clearly that the light breakout at the surface of this charge is not uniform. This fact indicates that the average detonation velocity cannot be constant along all charge radii. Moreover, the symmetric pattern of light breakout strongly suggests that there are preferred radial directions for detonation propagation within the charge. The only charge variables which change in a systematic fashion with radial direction are: (i) the distance travelled by the detonation front between discontinuities, (ii) the angle at which the detonation front contacts the discontinuity, and (iii) the number of discontinuities encountered. From this evidence, one can infer that the air gaps between the blocks may be influencing either the shape or rate of progress of the detonation front, or both.

3.0 DESCRIPTION OF EXPERIMENTS

3.1 EXPERIMENTAL PLAN

An objective of the present work was to investigate the origin of anomalous detonation propagation in large stacked charges composed of cast TNT blocks. It was, therefore, considered important to employ in the present study TNT blocks which were as close as possible to the original blocks in terms of dimensions, density, and crystal structure. To accomplish this goal, the original melting and cooling equipment and procedures used at DRES to prepare TNT blocks for the large-scale blast trials were employed.

The cast TNT block of dimensions 10.2cm x 30.5cm x 30.5cm, weighing approximately 15 kg, was adopted as the basic experimental charge. The experiments employing these blocks were designed to study the characteristics of detonation propagation between two or more blocks as a function of (i) geometry, (ii) gap size and (iii) confinement.

3.1.1 CHOICE OF EXPERIMENTAL GEOMETRIES

Inspection of the large charge cross-sections in Figures 2 and 3 reveals that block geometry encountered by a radially-propagating detonation front changes constantly as one moves from a radius in the equatorial plane to a radius along the vertical charge axis. Since it was not feasible to study all possible geometries, three distinct cases were chosen for study. These are shown in Figure 10.

The first case corresponds to a set of TNT blocks set end-to-end with the end surfaces (10.5 cm x 30.5 cm) touching and the detonation front proceeding normal to these surfaces. This configuration (Configuration 1) is encountered in the equatorial plane of the charge (directions 1 and 2 in Figure 3).

The second case corresponds to a simple stack of TNT blocks with the large side surfaces (30.5 cm x 30.5 cm) in contact, and the detonation front proceeding normal to these surfaces. This configuration (Configuration 2) is encountered along the vertical axis of the charge (direction 3 in Figure 2).

The final configuration chosen corresponds to a set of TNT blocks with

the 10.5 cm x 30.5 cm surfaces touching, one corner in common, and the detonation front proceeding diagonally through the blocks. This configuration (Configuration 3) is encountered in the median plane of the charge (directions 4 and 5 in Figure 3).

For both Configurations 1 and 2, the detonation front is parallel to the edge of the block as it crosses the interface between blocks (at least for blocks in large stacked charges at some distance from the point of initiation). In Configuration 1, the detonation front propagates across the long (30.5 cm) dimension of the block between discontinuities, whereas in Configuration 2, the front propagates across the narrow (10.5 cm) dimension between discontinuities. Case 3 is fundamentally different from Cases 1 and 2 in that the detonation front, propagating diagonally across the block, intersects the interface between blocks at an angle. In Case 3, as both the shock wave at the leading edge of the detonation front and gaseous detonation products behind the front enter the air gap, a component of the velocity of each will lie parallel to the block edge. In Configuration 3, therefore, some motion of the shock wave and detonation products along the channel between blocks created by the presence of the air gap might reasonably be expected.

3.1.2 CHOICE OF GAP SIZE

An inspection of photographs showing TNT blocks being laid in place in the 500 ton charges reveals that most blocks are emplaced carefully enough that the gap width between blocks is essentially zero. Occasionally, however, gaps of up to 12 mm can occur between blocks; gaps of order 6 mm are more common, and gaps of 25 mm represent an upper limit.

Previous work at DRES, reported by Holsgrove⁵, studied detonation transfer between the same cast TNT blocks for air gap sizes in one inch steps from 25 mm (1 inch) up to 280 mm (11 inches), in a configuration corresponding to Configuration 1 above. In the present study, gaps up to 76 mm (3 inches) were studied in Configuration 1 to provide a point of contact with Holsgrove's work. For Configuration 2 and 3, gaps up to 25 mm were studied, since it was felt that

most of the air gaps encountered in the large stacked charges were likely to fall within this range.

3.1.3 CHOICE OF CONFINEMENT MEDIUM

On the interior of the large block-built TNT charges, detonation in a particular block was effectively confined by the surrounding TNT blocks. An ideal experimental configuration for the present work would consist of a donor and receptor block surrounded completely by other TNT blocks. However, such a configuration would have resulted in an excessively-large explosive charge, and, since the confining TNT blocks are opaque, would not have permitted the use of ultra-high speed photography to document the progress of the detonation front through the interior blocks. The next most desirable situation would require that the confining TNT blocks be replaced by a transparent inert material having exactly the same mechanical response as TNT. Such a material could not be identified. 19 mm thick transparent plexiglass sheet was selected as the best compromise material. It has an acoustic impedance lower than that of TNT, so strong shock reflections at the interfaces should not be a factor.

4.0 EXPERIMENTAL TECHNIQUE

4.1 GENERAL

Each experiment consisted of a single donor block and between one and three receptor blocks. The blocks were organized in one of three geometries, corresponding to Configurations 1 through 3 of Figure 10. The donor blocks were simultaneously initiated across a planar surface 10.5 cm in depth by 30.5 cm in width. This was accomplished using an explosive plane-wave generator of the 'mousetrap' variety, described in Annex B. The plane-wave generator produced a detonation wave with a simultaneity of time of arrival on the initiation surface of 1 μ sec. This corresponds to a wave that is planar over the initiation surface to within 7 mm.

Detonation velocity in the donor and receptor blocks was measured in two ways:

- (1) streak photographs were recorded using a Cordin Model 330A ultra-high speed camera (this camera produces a simultaneous streak and framing record on the same time base).
- (2) for Configurations 1 and 2 (where the detonation front was expected to lie parallel to the block edge across the interface), resistive detonation velocity probes were cast into the interior of the charge normal to the expected direction of the detonation front.

4.2 CHARGE PREPARATION PROCEDURE

4.2.1 CASTING OF TNT BLOCKS

The TNT block used in the experiments was a cast rectangular block of dimensions 10.2 cm x 30.5 cm x 30.5 cm (4 in. x 12 in. x 12 in.) with a weight of 15 kg (33 pounds) and a bulk density of 1.59 g/cc. The blocks were formed by pouring molten TNT into rectangular molds made of 6 mm and 9 mm aluminum plate (shown in Figure 11). The casting procedure is described fully in Annex A.

4.2.2 CASTING OF RESISTIVE DETONATION VELOCITY PROBES INTO TNT BLOCKS

In order to permit detonation velocity measurements to be made in the interior of the block, a technique was developed to permit continuous resistive detonation velocity probes to be cast directly into the TNT blocks. A picture of three of these probes, suspended in a mold prior to casting the TNT block, is shown in Figure 12. A description of the resistive detonation velocity probe system is presented in Annex B.

4.2.3 CUTTING OF TNT BLOCKS

Configurations 1 through 3 shown in Figure 10 represent the desired experimental configurations. To limit the total quantity of explosive used in each experiment, full TNT blocks were cast, but only a portion of each block was

used in a given experiment. Figure 13 shows Configurations 1 through 3 from Figure 10 (represented by dashed lines). The solid lines in this figure represent the portions of the full blocks which were actually used in the experiments. The blocks were cut using a steam knife, as shown in Figure 14. In the set-up of the experiments, the blocks were arranged so that surfaces at the interfaces between blocks were not cut surfaces, but were the original surfaces produced in the mold.

4.2.4 PREPARATION OF EXPERIMENTAL CHARGE

Scotchlite* reflective sheeting (silver Scotchlite) was glued to the front surface of the TNT blocks. The purpose of the Scotchlite was to provide a highly-reflective surface which, when employed in conjunction with a high intensity flash illumination system, would render the front surface of the TNT blocks visible on the ultra-high speed photographic records to facilitate data analysis and interpretation.

The charges were mounted on a styrofoam stand with the center of the charge approximately 1.7 m (5.5 ft) above the ground surface. Styrofoam was used to minimize the ground shock transmitted to the camera bunker as a result of the coupling between the charge and the ground during detonation.

The charges were arranged with the initiation surface at the top to facilitate attachment of the explosive plane wave generator to the experimental charge. Balsa wood spacers were used to provide the required air gap separation between blocks. Their location and size were chosen so as to minimize their effect on the phenomenon under study.

An example of a four-block experiment (Configuration 3), set up and ready for firing, can be seen in Figure 15.

*Trademark of 3M Company

4.3 INSTRUMENTATION

4.3.1 ULTRA-HIGH SPEED PHOTOGRAPHY

The ultra-high speed photographic records were provided by a Cordin Model 330A streak and framing camera (Figure 16). This camera provides a simultaneous streak and framing record on the same time base. It is a rotating-mirror camera with a maximum framing rate of 2×10^6 frames/second (streak writing rate of $10.64 \text{ mm}/\mu\text{sec}$). The framing rate employed in the present set of experiments varied from 0.8 to 1.38×10^6 frames/second. The film employed was Kodak ASA 200 colour positive film. The camera was housed in a fortified bunker designed to permit the photography of charges as large as 58 kg (128 pounds) of TNT from distances as close as 21.3 m (70 feet). Most of the charges studied in the report were photographed from a distance of 27.5 m (90 feet) using a lens system with an overall focal length of 720 mm.

A lead vapour shutter⁸ with a closing time of approximately $10 \mu\text{sec}$ was used to provide rapid shuttering of the detonation event in order to prevent optical overwrite. The front surface of the charge, covered with Scotchlite, was illuminated by a collimated beam from a high-intensity Xenon flashlamp. A special arrangement of mirrors⁹ was used to optimize the amount of light returned to the camera after reflection from the Scotchlite surface. Detonation of the explosive charge, and triggering of the rapid shutter and flashlamp, were synchronized through a Cordin Model 453 three-channel time-delay generator. The time-delay generator channels, were, in turn, triggered by the FIRE pulse generated by pushing the FIRE button on the Cordin camera control console. The camera was operated in MANUAL mode; in this mode the camera operator activates the firing sequence manually by pushing the FIRE button once he is satisfied that the rotating mirror period on the camera has stabilized at a pre-set value.

A full description of the ultra-high speed photographic field laboratory, including the Cordin camera, Xenon flash illumination source and associated optics, rapid shutter system, and synchronizing electronics, can be found in Reference 9. A plan view of the camera layout is given in Figure 17.

4.3.2 CONTINUOUS RESISTIVE DETONATION VELOCITY PROBES

For Configurations 1 and 2, where the detonation front was expected to proceed through the block more or less parallel to the block edge, sets of continuous resistive-type detonation velocity probes were cast into the interior of the TNT blocks normal to the expected direction of travel of the detonation front. The principle of operation of these probes is described in Annex C.

A diagram showing the positions and dimensions of the probes used for Configurations 1 and 2 is presented in Figure 18. The output signal from each probe (voltage vs. time) was stored in a multichannel digital transient waveform recorder manufactured by Physical Data, Inc., then transferred to a Tektronix 4052 desktop computer for analysis.

5.0 DATA ANALYSIS TECHNIQUES

5.1 FRAMING RECORD

The 35 mm framing records were projected at x20 optical magnification onto the platen of a Telereadex film reader, one frame at a time. Using the outline of the TNT blocks to register each frame, a tracing of the position of the detonation front for each frame was made onto a single sheet of drawing paper.

This technique produced a composite picture of the progress of the detonation front through the TNT blocks as shown in Figure 19. Digital information was then extracted from this composite drawing.

To determine propagation velocity along a selected line in the charge or air gap, the drawing was oriented on the platen so that the Y (horizontal) cross-hair was aligned with the direction of interest. One dimensional position-time data were produced by using the X (vertical) cross-hair to determine the digital co-ordinates of the points of intersection of the horizontal cross-hair with successive positions of the detonation fronts. The time axis was established using a constant interframe time derived from the measured period of the rotating

mirror on the Cordin Model 330A Camera. The distance scale was established using the known dimensions of the front surfaces of the TNT blocks.

5.2 STREAK RECORD

The leading edge of the 35 mm streak records was digitized manually using a Telereadex film reader. The digitized co-ordinates were transferred on-line to a Tektronix 4052 computer for subsequent analysis. A time calibration for the X-axis was established using the information, provided by the camera manufacturer, that the mirror turbine speed which produces a framing rate of one million frames/sec corresponds to a steak writing rate of 5.23 mm/ μ sec. A distance calibration for the Y-axis was established using the images of the Scotchlite-covered front faces of the TNT blocks recorded on the streak film.

A typical digitized distance vs. time record is shown in Figure 20. The records generally could be broken down into segments, some of which were linear and some of which had definite curvature.

Using a standard least squares fitting procedure¹⁰, a straight line was fit to the linear segments and a quadratic or cubic polynomial was fit to the curved segments. Detonation velocity as a function of time was obtained for each segment by differentiating the fitting polynomial with respect to time.

5.3 RESISTIVE DETONATION VELOCITY PROBE

Analog output signals from the resistive detonation velocity probes were digitized and stored in a digital transient waveform recorder. The digitized records of voltage vs. time were transferred to a Tektronix 4052 computer for subsequent analysis.

After subtracting the baseline voltage and applying appropriate calibration constants, a distance vs. time plot was obtained, as shown in Figure 21.

Using the same least squares fitting procedure as applied to the streak records, the probe records were divided into one or more straight-line segments,

each fit by a linear polynomial. Detonation velocity as a function of time was obtained for each segment by differentiating the fitting polynomial with respect to time.

5.4 ESTIMATION OF ERROR

Each of the detonation velocities quoted in this report was derived as the slope of a linear fit to position-time data. The standard deviation in the slope, as determined through the fitting procedure from the scatter in the data about the best-fit curve, was taken as the experimental error in detonation velocity. When an average velocity was obtained by averaging two or more individual velocities, the following formulae were employed to calculate \bar{v} , the average velocity, and σ , the standard deviation of \bar{v} :

$$\bar{v} = \frac{\sum_i (v_i / \sigma_i^2)}{\sum_i (1 / \sigma_i^2)} \qquad \sigma = \left[1 / \sum_i (1 / \sigma_i^2) \right]^{1/2}$$

where v_i is an individual velocity estimate and σ_i its standard deviation.

In the following text, detonation velocity and standard deviation are frequently quoted together as, for example, 6.50 (0.15) km/sec. In this example, the estimated velocity is 6.50 km/sec and the associated standard deviation is 0.15 km/sec.

6.0 DISCUSSION OF RESULTS

Results for Configurations 1 and 2 are presented and discussed separately. In cases where the detonation velocities recorded by the three resistive probes within a donor or receptor block agreed within experimental

error, the results were averaged and a single value for the detonation velocity was reported for that block. In cases where the detonation velocity from an individual probe appeared anomalously low or high, a decision as to whether to retain or reject the data point was based upon the quality of the record as well as the extent to which the point deviated from the average of the remaining data points.

Table 1 presents detonation velocities measured in donor and receptor blocks for Configuration 1 (see Figure 13). Results for three experiments employing TNT blocks in Configuration 1 confined by 19 mm of plexiglass sheet are also presented in this table. Table 2 presents detonation velocities measured in donor and receptor blocks for Configuration 2.

The constant detonation velocities recorded in Tables 1 and 2 for unconfined TNT blocks in Configurations 1 and 2 are plotted in Figures 22 and 24 respectively. To permit intercomparison of results, in these figures the results from the individual experiments are plotted in sequence, in order of increasing air gap size. Lines representing the edges of the donor and receptor blocks have also been drawn.

6.1 CONFIGURATION 1 (TWO TNT BLOCKS)

The horizontal dashed line in Figure 22 represents a detonation velocity of 6.52 (0.08) km/sec obtained by averaging results for donor blocks from all Configuration 1 experiments without confinement. The detonation velocities measured in the donor blocks all lie within one standard deviation of this value. Moreover, the detonation velocities obtained from the streak and probe records from individual experiments agree within experimental error in those experiments where both types of records are available.

With regard to results in the receptor blocks, two distinct cases exist. In the first case (0 mm, 13 mm, and 25 mm air gaps), the detonation velocity is constant throughout the entire receptor block, and agrees within experimental error with the average detonation velocity measured for the donor blocks. In the second case (6 mm, 50 mm and 75 mm air gaps), the probe records from the interior of the receptor block indicate a constant velocity within the block, while the

streak records recorded from the surface of the block indicate two distinct velocities - a constant low-order velocity for the first 50 mm followed by an abrupt transition to a constant high-order velocity in the remainder of the block. The high-order velocity agrees within experimental error with the high-order velocity measured on the interior of the block. If the low-order velocities are ignored and the remaining detonation velocities recorded in the receptor blocks for all six Configuration 1 unconfined experiments are averaged, the resultant value of 6.60 (0.11) km/sec agrees with the corresponding value in the donor blocks within experimental error.

Figure 23 shows a plot of results from three experiments conducted employing two TNT blocks, in Configuration 1, confined in a box consisting of 19 mm thick plexiglass. The average detonation velocity recorded in the donor blocks for this series was 6.37 (0.18) km/sec, a value which is lower than the average detonation velocity in the unconfined donor blocks, but consistent within experimental error. In the confined receptor blocks, two of the velocities obtained from streak records, 7.76 (0.44) and 8.28 (0.30), were not physically reasonable. The remaining detonation velocities were uniformly higher than in the donor blocks, but were still within two standard deviations of the average value in the donor blocks. Confinement by 19 mm plexiglass did not result in a statistically significant increase in detonation velocity in the donor-receptor system.

6.2 CONFIGURATION 2 (TWO TNT BLOCKS)

The horizontal dashed line in Figure 24 represents a detonation velocity of 6.23 (0.07) km/sec obtained by averaging results in identical unconfined donor blocks from five separate Configuration 2 experiments. This value is four standard deviations lower than the corresponding average value from six Configuration 1 experiments. The donor blocks for Configuration 1 and Configuration 2 experiments were prepared using identical procedures and were initiated using identical plane-wave generator systems.

The principal difference in the two configurations lies in the direction of detonation propagation with respect to the crystal axes within the TNT blocks. Figure 7 shows clearly the pattern of large elongated crystals found within the TNT blocks. In Configuration 1, the velocity vector of the detonation front is

perpendicular to the long axis of the TNT crystals. In Configuration 2, the velocity vector is parallel to the long crystal axis.

The present results support the conclusion that the value of the stable detonation velocity in the cast TNT blocks is influenced by crystal orientation within the blocks. This effect has been noted by other workers^{11, 12} and is discussed further in Section 6.4.

High order detonation transferred successfully into the unconfined Configuration 2 receptor blocks for air gaps up to 25 mm. For each experiment in the series, the streak and resistive probe measurements of stable detonation velocity in the receptor block agree within experimental error. However, when these values are averaged for each block, the resultant does not always agree within error with the overall average of 6.23 (0.07) km/sec from five donor blocks (dashed line). In two cases (6 mm and 13 mm air gap), the average detonation velocity in the receptor block is higher than the average value in the donor blocks. The larger scatter in results observed for Configuration 2 receptor blocks, when compared to results for Configuration 1 receptor blocks, may be a further manifestation of the influence of crystal structure on detonation propagation.

The results from donor and receptor blocks, taken together, suggest that detonation propagation in the cast TNT blocks is more difficult when the propagation velocity vector is parallel to the long axis of the TNT crystals.

6.3 CONFIGURATION 3 (FOUR TNT BLOCKS)

Results from Configuration 3 experiments are summarized in Figures 25 through 29 and in Table 3. Figure 25 shows a composite set of tracings of the detonation front position, extracted from the framing records for experiments with 3 mm, 13 mm, and 25 mm air gaps. The TNT blocks were unconfined. The following qualitative observations can be made:

- (i) For receptor blocks A and B, the initial direction in which the detonation front propagates in the blocks is a function of gap width. The

propagation direction becomes more nearly normal to the block edge as the gap width is increased.

(ii) Luminous detonation product gases channel ahead of the detonation front.

(iii) The hot channelled gases give rise to reaction waves in receptor block C which initially move approximately perpendicular to the surfaces of that block and meet at an interior point in the block. From the point of intersection, a detonation wave emerges moving more or less parallel to the original detonation front in the donor block. The point at which this detonation front re-establishes itself in receptor block C is dependent upon the gap width.

In Figure 26, superposed on the tracings of Figure 25 are solid straight lines, along the charge diagonal and in the air gaps, along which constant propagation velocity was measured. The position and length of each line denote a region of stable propagation velocity. The constant velocities which were measured are listed in Table 3. For all three experiments, the stable detonation velocities in donor and receptor block agree within experimental error except for the value in the receptor block for the three millimeter gap configuration, which is anomalously low. With reference to air gaps 1 through 4*, the results indicate that the stable propagation velocities of the detonation products in air gaps 1 and 2 agree within experimental error, as would be expected from symmetry considerations. The measured values tend to decrease in moving from the 3 mm to 25 mm air gap, but this variation is not statistically significant, given the relatively large experimental uncertainties. The stable propagation velocities of the detonation products in gaps 3 and 4 again agree within experimental error. The measured values are largest for the 3 mm gap, and smallest for the 25 mm gap, but the experimental uncertainties are again too large to claim that this trend is statistically significant.

*For numeric designation of air gaps, see diagram accompanying Table 3.

Figures 27 through 29 present a more detailed analysis of selected fronts from the framing records of Figure 25. A grid of dotted lines superposed on the donor block represents successive positions of an "ideal" detonation front propagating exactly parallel to the initiation surface (at an angle of 45° to the block edge). The angle formed by the intersection of these lines with the initial plane of the detonation front in receptor blocks A and B is indicated on the drawing. These measurements reveal that the angle between the initial propagation direction in the receptor block and the original propagation direction in the donor block is non-zero and increases from approximately 16° to 20° to 23° as the air gap width increases from 3 mm to 13 mm to 25 mm, respectively. For an ideal case (continuous block with no air gap), this angle would be zero. Thus one effect of the air gap is to change the initial direction of detonation propagation in adjacent receptor blocks. This effect becomes more pronounced as the gap width is increased. In all cases examined, the propagation direction appears to change gradually back to a direction close to that in the donor block as the front advances into the receptor block. However, the receptor blocks were not large enough in the present experiments to establish if the original propagation direction would be completely restored.

Also included in Figures 27 through 29 are straight lines, superimposed on receptor block C, which represent predicted positions for the detonation front if the air gaps were not present. In formulating these predictions, the measured stable detonation velocity in the respective donor block was employed. The error bar on the predicted position reflects the uncertainty in the measured detonation velocity. Also shown on Figures 27 through 29 are the actual detonation front positions observed on the framing records. For the 3 mm air gap, the actual front position lags the "predicted" position, by one standard deviation. For 13 and 25 mm air gaps, the actual front position also lags the predicted position. The lag is well outside experimental error and is largest for the 25 mm air gap. From these results, it can be concluded that the air gap not only alters the initial shape of the detonation front in receptor block C, but also causes a delay in the re-establishment of a stable detonation in that block. The delay increases with air gap width, being less than $2 \mu\text{sec}$ for a 3 mm air gap and of order $9 \mu\text{sec}$ for a 25 mm air gap.

It is also clear from an examination of Figures 25 through 29 that the initial shape of the detonation wave in receptor block C is strongly influenced by the width of the air gap. The results, taken together, are consistent with a picture in which hot, high pressure detonation products channel ahead of the main detonation front in the donor block. They move into the gaps adjacent to receptor block C. The pressure and temperature in the channeled detonation products at the block surfaces with which they are in contact are sufficiently high to induce a reaction wave at these surfaces. Since two surfaces are involved, two reaction waves are created, moving initially at right angles to the block surfaces. At a point on the interior of the block, these two waves intersect. From the point of intersection, a high order detonation wave emerges, with velocity vector parallel to the bisector of the angle of intersection and approximately parallel to the velocity vector of the detonation front in the donor block. The width of the front grows as it proceeds through the block. The similarity between the observed process and the process of Mach stem formation following the collision of symmetric strong shock waves is striking.

An accurate measurement of the velocity of propagation of the laterally-moving reaction waves in the receptor block could not be made due to the constantly changing shape of these waves and limited number of data points. However, for the 25 mm air gap experiment, it was possible to establish an approximate average velocity of 3.8 km/sec. This value is somewhat lower than, but close to, the stable low order detonation velocity of 4.3 km/sec recorded in cast TNT by Allen et al.¹³

When the above experiments were repeated with the blocks confined in a plexiglass box, the results were qualitatively similar to the results obtained with unconfined TNT blocks. Quantitative analysis was complicated by two factors: the low reflected light level from the Scotchlite surface when covered with 19 mm of plexiglass, and a tendency for the detonation products to channel ahead of the detonation front at points where a small air gap existed between the surfaces of the Scotchlite and plexiglass. Constant propagation velocities recorded in these experiments are listed in Table 3 for the sake of completeness, but a detailed quantitative analysis of these experiments has not been attempted due to the above limitations.

As in the two-block experiments, the addition of 19 mm plexiglass confinement did not alter significantly the measured detonation velocity in the donor block. Furthermore, the temporary distortion of detonation front shape in receptor block C was still present, but the re-establishment of a planar detonation wave occurred earlier in this receptor block when confinement was present (20 mm from the block corner with confinement and 65 mm from the block corner without confinement, for the experiment with 25 mm air gap). This change may be attributable to higher pressures in the channeled detonation products due to confinement.

6.4 RESULTS OF OTHER WORKERS

6.4.1 TWO-BLOCK CONFIGURATIONS (PARALLEL INCIDENCE)

In Reference 5, Holsgrove reported results from a series of experiments conducted at DRES in 1961 to study the ability of a detonation front to propagate between two cast TNT blocks. The blocks used in the 1961 experiments were identical to the ones used in the present experiments. The experimental configuration used by Holsgrove, shown in Figure 30, corresponds to Configuration 1 for the present experiments, with two exceptions. First, the experiments analyzed by Holsgrove employed full, rather than half, TNT blocks. Secondly, a 7 oz. hemispherical tetrytol primer was employed, initiated by a No. 8 Seismocap on one face of the donor block, rather than the planar initiation system with tetrytol booster slab used in the present experiments. The experiments described by Holsgrove employed ionization probes set into one face of the receptor block along the centre line. The detonation velocities measured were average velocities recorded between successive probe positions. Air gaps from one inch to eleven inches, in one inch steps, were examined; one experiment was performed at each gap distance. The results of these experiments are summarized in Figure 31. In general, as the gap size was increased, the initial velocity in the second block decreased and the run distance (distance to re-establish a stable high-order detonation velocity in the second block) was increased.

The detonation velocities recorded by Holsgrove for air gaps from one to three inches are reported in Table 4. Also included is a set of detonation velocities recorded from a single experiment employing a donor block.

It is clear that, for each gap distance, the detonation velocity at Position 1 is lower than the velocities at Positions 2 and 3. The velocities recorded at Positions 2 and 3 are equal to within 1.5%, a fact which confirms that the velocity is stable over the recording intervals represented by these points. Column 4 records the average of the velocities from Positions 2 and 3. Since the stable detonation velocities recorded in Column 4 are the same to within three percent for each gap width, these velocities are averaged in Column 5. The average value of 6.55 from the receptor blocks agrees with the stable velocity measured in the donor block to within 1 percent.

In the present experiments, for the donor blocks an average detonation velocity of 6.52 (.08) km/sec (average of streak and resistive probe records from six experiments) was obtained. Holsgrove's single measurement of 6.61 km/sec in the donor block falls almost within one standard deviation of this value. In the present experiments, for the receptor blocks an average detonation velocity of 6.60 (0.11) km/sec was recorded (average of streak and resistive probe records from six experiments involving six separate gap distances up to 75 mm). This compares with Holsgrove's average value of 6.55 km/sec for the detonation velocity in the receptor blocks. It is concluded that Holsgrove's measurements of detonation velocity are in good agreement with the present work.

6.4.2 EFFECT OF CRYSTAL ORIENTATION

Cybulski et al.¹¹ reported results of experiments to determine the velocity of detonation in cylinders of cast TNT. The TNT was prepared using four different pouring methods: (1) 'clear-poured', (2) 'poured-cloudy' or 'turbid-poured', (3) 'creamed' or 'creamy-poured' and (4) axially-crystallized. Methods (1) and (4) produced large coarse crystals with the long axis oriented perpendicular to the cylinder axis (radially-crystallized) and parallel to the crystal axis (axially-crystallized) respectively. It was found that the axially-crystallized TNT could not be detonated unconfined even with a powerful primer.

The radially-crystallized TNT from some batches could be detonated without confinement while the TNT from other batches could not. Streak photography revealed that the detonation front in the axially-crystallized TNT was unstable. By contrast, methods (2) and (3) above produced TNT with a relatively fine-grained crystal structure. The poured-cloudy and creamed castings could always be detonated unconfined; streak photography revealed a stable detonation front. The fact that fine-grained TNT is more sensitive to initiation than coarse-grained TNT has been verified by many workers. However, Cybulski's work also established clearly that detonation propagation is more difficult in coarse-grained TNT when the velocity vector is parallel to the long crystal axis. Further work reported in the same paper to determine the 'infinite-diameter' detonation velocity in axially-crystallized TNT was approximately 6% lower than the corresponding parameter in radially-crystallized TNT. Since the densities of these two forms of clear-poured TNT were almost equal, Cybulski concluded that "...the results suggest that there are characteristic values for the velocity of detonation according to the orientation of the crystals with respect to the direction of propagation."

Kegler¹² studied the detonation characteristics of clear-poured TNT in cylinders of 22 mm diameter cast in glass tubes with a wall thickness of 1.2 mm. By cooling in water, he obtained radially-crystallized samples. By cooling in air, he obtained considerably larger crystallites oriented partly irregularly and partly axially. The radially-crystallized samples detonated satisfactorily. No detonation could be induced in the air-cooled samples having a mixture of irregular and axial orientation. When cylinders of larger diameter (32 to 43 mm) were employed, the air-cooled samples (irregular plus axial orientation) produced either no stable detonation, or a velocity distinctly lower than in the case of radially-crystallized TNT.

The present experiments with coarse-grained TNT blocks agree with the findings of both Cybulski and Kegler. Measured propagation velocity was 5% lower and results in receptor blocks were more widely scattered when the propagation velocity vector was parallel to the long crystal axis.

6.4.3 FOUR-BLOCK CONFIGURATION (OBLIQUE INCIDENCE)

Most of the work reported in the literature on detonation propagation across air gaps in solid explosives concerns two units of explosive (donor and receptor), usually cylindrical, set end to end and separated by an air gap of controlled width (the geometry of the so-called air gap sensitivity test). In this geometry, the detonation front in the donor and receptor blocks is more or less parallel to the end of the cylinder. The geometry is similar to that of Configurations 1 and 2 in the present work (see Figure 13). No reference could be found in the literature to work on detonation propagation across air gaps in solid explosives for complex air gap geometries, i.e., for cases in which the detonation front intersected the interface between the explosive and the air gap at an angle (oblique incidence). The most relevant work seemed to be work on the internal channel effect reported by Woodhead and Titman¹⁴ and Ahrens¹⁵, summarized in Johansson and Persson's book, Detonics of High Explosives¹⁶. A brief summary of relevant results concerning the internal channel effect is now presented.

6.4.3.1 Internal Channel Effect

The following quotation is taken from Reference 16, page 68:

"If a cylindrical charge has an internal axial channel, the detonation is accompanied by a flow of gas in the channel that strongly affects the detonation process. The air enclosed in the channel is driven forward by the detonation gases in a compressed layer with a high temperature, high pressure, and a steep shock front. The gas compresses the explosive in front of the detonation front, and as a result of the increased density, the detonation velocity becomes greater than that obtained in an unconfined homogeneous cylindrical charge with the same initial density. In tubular charges of high explosives with a small initial density ($\rho_0 < 1 \text{ g/cm}^3$), this is the dominant effect. In more sensitive explosives, e.g. PETN, the gas flow causes an increase in the detonation velocity exceeding that caused by the increase in density".

A simple model for the channel effect taken from Reference 14 is presented in Figure 32. In this model, the detonation front acts as a driving piston, compressing and propelling a column of gas before it. If one used the shock front velocity w to calculate ρ_1/ρ_0 , the density ratio for a shock front with velocity w , then the particle velocity u of the compressed gas is given by the relation

$$u = (1 - \rho_0/\rho_1) w \quad (1)$$

If one carries out this calculation for a low-density explosive, e.g. loosely-packed tetryl with a density of 0.93 g/cm^3 , one finds that the particle velocity u of the compressed gas is approximately equal to the detonation velocity. This fact is consistent with the picture of the detonation front acting as a piston and pushing a column of compressed gas before it. However, if one performs the same calculation for a higher density explosive like cast TNT, tetryl, or PETN, one finds that the measured velocity of the compressed gas column is considerably greater than the values calculated assuming the detonation front as a driving piston, i.e. assuming $u = D$. The most probable explanation for this discrepancy, according to Reference 16, is the occurrence of chemical reaction and additional energy release to the gas column from the compressed explosive lining the gas column ahead of the detonation front. Further evidence for the occurrence of laterally-moving reaction waves in the bulk explosive ahead of the main detonation front is provided by the experimental observations reported by Ahrens¹³ and summarized in Figure 33. In this figure, D_c represents the largest detonation velocity that is possible in steady-state detonation (for a density corresponding to the crystal density). The open circles represent detonation velocities measured at three different explosive densities for homogeneous cylinders with an outside diameter d of 21 mm. The squares represent measurements at these same densities of detonation velocities, D_t , for tubular charges with an outside diameter of 21 mm and an internal channel diameter of 4 mm. The results indicate that the presence of the internal channel substantially increases the measured detonation velocity. In the case of tetryl and

PETN, the measured detonation velocities actually exceed D_c . As D_c is the largest detonation velocity that is possible in steady state detonation for that explosive, the fact that $D_t > D_c$ implies that the flow of the hot high pressure gas column along the inner surface of the explosive must be giving rise to a laterally-moving compression wave ahead of the detonation front which precompresses and preheats the explosive column and results in an increase in detonation velocity parallel to the charge axis.

6.4.3.2 Relation to Present Work

In the present work with four blocks of TNT, phenomena qualitatively similar to those in the internal channel effect were observed. Luminous gases were observed to move ahead of the detonation front in the channel created by the air gap. Recorded velocities of these gases were well above the stable detonation velocity in the TNT donor block. In the vertically-opposite receptor block, low-velocity reaction waves initiated by the hot gases at the block surfaces were observed to propagate into the TNT block ahead of the main detonation front. High order detonation in the block was re-initiated at the point where these waves intersected. It is felt that the phenomena observed in the four-block configuration in the present experiments are manifestations of the channel effect.

7.0 CONCLUSIONS AND RECOMMENDATIONS

Air gaps between large cast TNT blocks can influence both the shape and rate of propagation of an initially-stable detonation front proceeding through the blocks. When the detonation front is parallel to the block edge, the air gap leaves the shape of the front in the receptor block unaffected. Detonation propagates successfully across air gaps up to 75 mm. Results are basically unaltered when the blocks are confined by 19 mm of plexiglass. The TNT blocks

studied in this report had an ordered crystal structure featuring large elongated crystals. Detonation velocity was 5% higher in the donor blocks, and results in the receptor blocks less scattered, when the detonation proceeded across, rather than along, the long crystal axis. The results are consistent with a picture in which detonation propagation is favoured perpendicular to, rather than parallel to, the long crystal axis. When the detonation front encountered an air gap at an angle of 45° , luminous gases were observed to channel ahead of the front in the air gap, initiating reaction in adjacent blocks. At a corner between four blocks, the channelled gases initiated low-velocity reaction waves along two surfaces in the block vertically opposite the donor block. From the point of intersection of these two waves, a planar detonation front emerged, travelling approximately parallel to the original front in the donor block, but delayed with respect to that front. The delay increased with the width of the air gap. The delay was reduced somewhat when the blocks were confined by 19 mm of plexiglass.

Implications for Large Block-Built TNT Charges

The TNT blocks studied in the present experiments were identical to those employed in large-scale (500 ton) TNT charges detonated at DRES between 1958 and 1970. The present results provide direct experimental evidence that air gaps between the blocks can provide a local distortion of the shape and also a local delay in propagation of the detonation front. The effects are most pronounced when the detonation front enters the air gap at an angle, and increase as the air gap width increases.

Most of the air gaps in the large-scale TNT charges were 3 mm or less in width. Based on the present work, the author feels that such small air gaps probably would not play a significant role in the generation of blast anomalies. It is considered more likely that the occasional large air gap (3 mm - 25 mm, caused by imperfect block placement), may have contributed to the anomalies by acting as the trigger for creation of a Taylor instability. However, the possibility that a small perturbation at each boundary might have a large cumulative effect cannot be dismissed on the basis of the present work, since the geometries encountered within the large stacked charges are much more varied and complex than examined here.

The fact that a five percent difference in detonation velocity was observed depending upon whether the front was propagating perpendicular to, or parallel to, the long crystal axis implies that crystal structure within the TNT block might also have contributed to non-uniform shock waves from the large stacked charges, by creating preferred directions for detonation propagation within the charge.

8.0 REFERENCES

1. Patterson, A.M., Kingery, C.N., Rowe, R.D., Petes, J. and Dewey, J.M., "Fireball and Shock Wave Anomalies", The Technical Cooperation Program Panel N-2 Technical Summary Report N2: TR 1-70, August 1970. UNCLASSIFIED.
2. Phillips, A.C., Ditto, W.J. and Holdsworth, J., "Building of Hemispheres of High Explosives from Cast Blocks", Suffield Technical Paper No. 194, 1962. UNCLASSIFIED.
3. Mader, C.L., "Initiation of Detonation by the Interaction of Shocks with Density Discontinuities", Physics of Fluids, 8, (1965) 1811.
4. Cook, M.A., The Science of High Explosives, Reinhold Publishing Corporation (New York), 1958.
5. Holsgrove, B.J., "Detonation of Stacked TNT Blocks - A Review of the Attenuating Effects of Air Gaps", Suffield Memorandum No. 7/68, 1968. UNCLASSIFIED.
6. Wisotski, J., "Test of Stacked TNT Blocks", 19th Monthly Report, Denver Research Institute, DRI No. 884-6711-M, 1967. UNCLASSIFIED.
7. Taylor, G., "The Instability of Liquid Surfaces when Accelerated in a Direction Perpendicular to their Planes", Proc. Roy. Soc. (London), A201, (1950) 192.

8. Gibb, A.W., Naylor, R., Nolan, M.A., and Dempsey, J.B., "Application of an Exploding Wire Capping Shutter to the Study of Solid High Explosive Charges Using an Ultra High-Speed Rotating Mirror Camera", Proceedings of 15th International Congress on High-Speed Photography and Photonics, San Diego, California, 21-27 August, 1982.
9. Gibb, A.W., Nolan, M.A., and Dempsey, J.B., "Portable Ultra High-Speed Photographic Field Laboratory Suitable for the Study of Self-Luminous and Nonluminous Detonations in Solid High Explosive Charges (10-130 Pound TNT Equivalent)", Proceedings of 15th International Congress on High-Speed Photography and Photonics, San Diego, California, 21-27 August, 1982.
10. Matthews, J. and Walker, R.L., Mathematical Methods of Physics, W.A. Benjamin, Inc. (New York), 1965.
11. Cybulski, W.B., Payman, W., and Woodhead, D.W., "Explosion Waves and Shock waves, VII. The Velocity of Detonation in Cast TNT", Proc. Roy. Soc. (London) A 197, (1949) 51.
12. Kegler, W., "Sensitization of Trinitrotoluene by Nitrocellulose and Other Additives", Explosivstoffe 11, (1963) 209.
13. Allen, H.J., Cook, M.A., and Pack, D.H., "Transients in Detonation", Technical Report No. L, Project Number 357 239, Institute for Study of Rate Processes, University of Utah, 1956. UNCLASSIFIED.
14. Woodhead, D.W. and Titman, H., "Detonation Phenomena in a Tubular Charge of Explosive", Explosivstoffe 13, (1965) 113, 141.
15. Ahrens, H. "Über den Detonationsvorgang bei Zylindrischen Sprengstoffladungen mit Axialer Höhlung", Explosivstoffe 13, (1965) 124, 155, 180, 267, 295.
16. Johansson, C.H. and Persson, P.A., Detonics of High Explosives, Academic Press (London), 1970.

UNCLASSIFIED

TABLE 1 - SUMMARY OF RESULTS FROM CONFIGURATION 1 EXPERIMENTS

EXPERIMENT DESCRIPTION	DETONATION VELOCITY (km/sec)			
	DONOR BLOCK		RECEPTOR BLOCK	
	Streak Camera Record	Resistive* Probe Record	Streak Camera Record	Resistive* Probe Record
A. Unconfined Blocks				
Air Gap 0 mm	not available	6.62 (0.17)	not available	6.30 (0.40)
Air Gap 6 mm	6.30 (0.24)	6.56 (0.23)	first 25 mm 4.72 (0.21) next 125 mm 6.91 (0.62)	6.66 (0.40)
Air Gap 13 mm	not available	6.78 (0.20)	not available	6.42 (0.56)
Air Gap 25 mm	6.03 (0.33)	not available	6.72 (0.34)	not available
Air Gap 50 mm	6.42 (0.19)	6.55 (0.23)	first 50 mm 3.91 (0.49) next 100 mm 6.59 (0.16)	6.28 (0.49)
Air Gap 75 mm	6.54 (0.46)	6.58 (0.43)**	first 50 mm 4.51 (0.33) next 100 mm 6.82 (0.48)	first 50 mm 4.98 (0.52) next 100 mm 6.72 (0.31)
B. Blocks confined by plexiglass				
Air Gap 3 mm	6.63 (0.65)	5.97(0.36)***	7.11 (0.35)	first 40 mm 4.30 (0.75) next 110 mm 6.76 (0.22)
Air Gap 13 mm	6.41 (0.68)	6.60(0.61)***	7.76 (0.44)	first 30 mm 3.72 (0.70) next 120 mm 6.88 (0.23)
Air Gap 25 mm	6.57 (0.36)	6.40 (0.36)	first 30 mm 3.87 (0.25) next 120 mm 8.28 (0.30)	

* All resistive probe results for a single block represent an average of three probe records, unless otherwise noted.

** Result from one probe only, centrally situated in block.

***Average of two probe records.

UNCLASSIFIED

UNCLASSIFIED

TABLE 2 - SUMMARY OF RESULTS FROM CONFIGURATION 2 EXPERIMENTS

EXPERIMENT DESCRIPTION	DETONATION VELOCITY (km/sec)			
	DONOR BLOCK		RECEPTOR BLOCK	
	Streak Camera Record	Resistive* Probe Record	Streak Camera Record	Resistive* Probe Record
Air Gap 0 mm	5.98 (0.18)	6.19 (0.42)	5.71 (0.15)	5.99 (0.46)
Air Gap 3 mm	not available	not available	not available	8.03 (1.38)
Air Gap 6 mm	5.85 (0.29)	6.44 (0.20)	first 20 mm 2.81 (0.16) next 80 mm 6.74 (0.38)	6.34 (0.43)
Air Gap 13 mm	6.11 (0.20)	7.10 (0.87)	first 40 mm 6.42 (0.56) next 60 mm 7.29 (0.28)	7.05 (0.80)
Air Gap 19 mm	6.45 (0.25)	6.10 (0.20)	6.14 (0.23)	5.72 (0.44)
Air Gap 25 mm	6.26 (0.17)	6.98 (0.33)	first 25 mm 4.01 (0.42) next 75 mm 5.68 (0.25)	6.26 (0.39)**

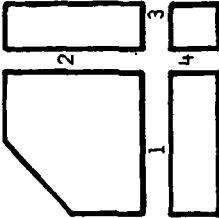
* All resistive probe results for a single block represent an average of three probe records, unless otherwise noted.

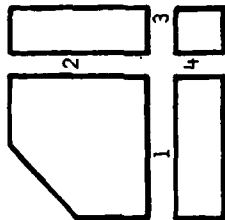
**Result from one probe only, centrally situated in block.

UNCLASSIFIED

UNCLASSIFIED

TABLE 3 - SUMMARY OF RESULTS FROM CONFIGURATION 3 EXPERIMENTS

EXPERIMENT DESCRIPTION	DETONATION VELOCITY (km/sec)					
	DONOR BLOCK	RECEPTOR BLOCK	GAP 1	GAP 2	GAP 3	GAP 4
A. UNCONFINED BLOCKS						
Air Gap 3 mm	6.73 (0.40)	5.91 (0.19)	9.55 (0.80)	9.97 (0.87)	10.0 (0.46)	9.45 (0.34)
Air Gap 13 mm	6.88 (0.42)	7.17 (0.50)	8.44 (0.33)	9.24 (0.94)	8.68 (1.13)	10.1 (0.93)
Air Gap 25 mm	6.60 (0.50)	6.99 (0.42)	8.76 (0.61)	8.96 (0.52)	8.76 (0.61)	8.96 (0.52)
						
B. BLOCKS CONFINED BY PLEXIGLASS						
Air Gap 13 mm	7.12 (1.01)	4.07 (0.36)	9.21 (0.89)	10.8 (1.08)	8.27 (1.05)	9.91 (0.64)
Air Gap 25 mm	6.68 (1.08)	3.93 (0.46)	9.16 (0.88)	9.19 (1.96)	8.45 (0.76)	6.81 (0.89)



UNCLASSIFIED

UNCLASSIFIED

TABLE 4 - DETONATION VELOCITIES FROM HOLSGROVE REPORT

Air Gap (mm)	Detonation Velocities (km/sec)				Average of Results in Column 4 for 3 gap distances
	Position 1	Position 2	Position 3	Average Position 2 + 3	
Donor Block	5.325**	6.546	6.667	6.606	} 6.553
25	6.496	6.667	6.667	6.667	
50	5.976	6.446	6.546	6.496	
75	5.173	6.446	6.546	6.496	

Position 1: 63.5 mm (midpoint of Sensors 1 and 2)

Position 2: 152 mm (midpoint of Sensors 2 and 3)

Position 3: 250 mm (midpoint of Sensors 3 and 4)

**Low value possibly due to inadequate boosting.

UNCLASSIFIED

UNCLASSIFIED

ANNEX A

DESCRIPTION OF CASTING PROCEDURE FOR TNT BLOCKS

The basic charge used in the experiments was a cast rectangular TNT block of dimensions 10.5 cm x 30.5 cm x 30.5 cm (4 in x 12 in x 12 in) with a weight of 15 kg (33 lb) and a bulk density of 1.59 g/cc. The blocks were cast using exactly the same procedure that was used to cast blocks for the large-scale trials at DRES between 1958 and 1970.

The blocks were formed by pouring molten TNT into rectangular molds made of 6 mm and 9 mm aluminum plate (Figure 11). Six molds were suspended in a cooling tank. A header of molten TNT was maintained above each mold to take up shrinkage as the material hardened. Once the TNT had been poured into the molds, the cooling tank was filled with water to a depth of 30 cm and water allowed to circulate freely for 45 minutes. At the end of this period, the tank was drained and the blocks were allowed a natural cooling time of 4.5 hours. Shrinkage of the TNT block upon solidifying was such that, after removing the bottom of the mold, the block would slide out. The result was a TNT block with smooth surfaces whose shape satisfied the following tolerances (according to Reference 2):

- (i) faces flat to within 0.05 inches
- (ii) large faces parallel to within 0.2° of arc
- (iii) mean distance between large faces $4" \pm 0.02"$
- (iv) edge faces parallel within 0.3° of arc
- (v) mean distance between edge faces $12" \pm 0.03"$
- (vi) adjoining faces at 90° within 0.3°

The projection on the block located where the header had entered the mold was removed by scraping with a knife.

UNCLASSIFIED

UNCLASSIFIED

ANNEX B

EXPLOSIVE PLANE-WAVE GENERATOR

A mousetrap-type explosive plane-wave generator was used to initiate the TNT blocks studied in this report. A sketch and photograph of this plane-wave generator are presented in Figure 34.

This type of plane-wave generator employs a detasheet line-wave generator (LWG) to convert the spherically-expanding detonation front (resulting from point initiation by a detonator) to a linear detonation front. The linear detonation front is then transferred to one end of a rectangular piece of 6 mm thick solid detasheet. The detasheet was confined on either side by two 6 mm thick sheets of ordinary window glass. This entire assembly was mounted at an angle of 12° on top of a 13 mm thick tetrytol booster block.

The mousetrap plane-wave generator functions as follows:

- (i) Point initiation by the detonator is converted to a linear detonation front by the line-wave generator.
- (ii) The linear detonation front propagates uniformly along the length of solid detasheet; the expanding product gases propel that part of the lower glass confining plate with which they are in contact toward the tetrytol booster pad.
- (iii) For a given explosive type and explosive/glass mass ratio, careful choice of the angle between the detonating assembly and tetrytol booster pad will produce a situation in which all of the glass particles impact the surface of the tetrytol pad virtually simultaneously. This results in uniform planar initiation of the tetrytol pad over its entire surface area.

In a real plane-wave generator, exact simultaneity of initiation over the entire initiation surface can never be fully realized. For the device described above, time-of-arrival measurements, made at the base of the tetrytol booster pad using ionization probes, revealed that the variation in detonation front time-of-

UNCLASSIFIED

arrival across the bottom surface of the booster pad was not more than 1.0 μ sec. For a detonation front propagating in a TNT block, with a detonation velocity of approximately 6.6 mm/ μ sec, this corresponds to a maximum departure from planarity of 7 mm across an initiation surface 100 mm x 300 mm. The relative delays in initiation time across the initiation surface result in minor changes in the initial shape of the detonation front, but do not affect the basic direction of propagation of the detonation front nor the measured detonation velocity.

It was found that two plywood supports (Figure 34) used to prop the plane-wave generator at the correct angle relative to the tetrytol booster pad, were very important to the performance of the device. It was discovered during the development process for this device that if these were removed and replaced with a single vertical strut, a high order detonation could not be initiated in the tetrytol pad. The lateral confinement afforded by these solid wooden panels was apparently crucial to the proper functioning of the device.

UNCLASSIFIED

ANNEX C

RESISTIVE DETONATION VELOCITY PROBE SYSTEM

The resistive type of detonation velocity probe is widely used in detonation research involving solid or liquid explosives to produce a continuous record of detonation velocity over some portion of a detonating explosive charge.

The probes used at DRES consisted of a length of high-resistance molycloy wire, with a resistance of 292 ohms/meter, inserted into a stainless steel tube of 1 mm outside diameter. The wire was wrapped with a single wrap of nylon insulation to provide electrical isolation between the molycloy wire and the stainless steel tube. One end of the stainless steel tube was crimped to provide electrical contact with the molycloy wire at that point. The other end of the stainless steel tube and molycloy wire, respectively, were linked to a constant current source which was designed to deliver 70 milliamperes of current through the probe, even in the presence of a rapidly-changing resistive load.

The probe was oriented with the crimped end facing the expected direction of advance of the detonation front. As the detonation front advanced along the probe, the very large pressure associated with the front collapsed the outer tube against the inner wire, progressively shorting the probe and producing a continuously-changing resistance. This continuously-changing resistance was detected as a continuously-changing voltage across the probe. The probe output (voltage vs time) was recorded on a digital transient waveform recorder at a digital sampling rate of two million samples per second.

A precise time base was established for each record using the constant sample rate of 0.5 μ sec/sample provided in the digitizing process. In order to extract detonation velocity from the probe record, it was necessary to convert the Y coordinates from voltage units to distance units. This was accomplished through application of Ohm's law

$$\Delta V = -i_0 (dR/dx) \Delta x$$

UNCLASSIFIED

where ΔV is voltage change in volts
 i_0 is the (constant) current of 70 mA running through the probe
 dR/dx is the resistance per unit length of the molycloy wire +
stainless steel tube (0.292 ohms/mm)
 Δx is distance along the probe in mm, measured from the crimped end of
the probe.

An example of a typical digitized distance vs time record from the probe system can be seen in Figure 21.

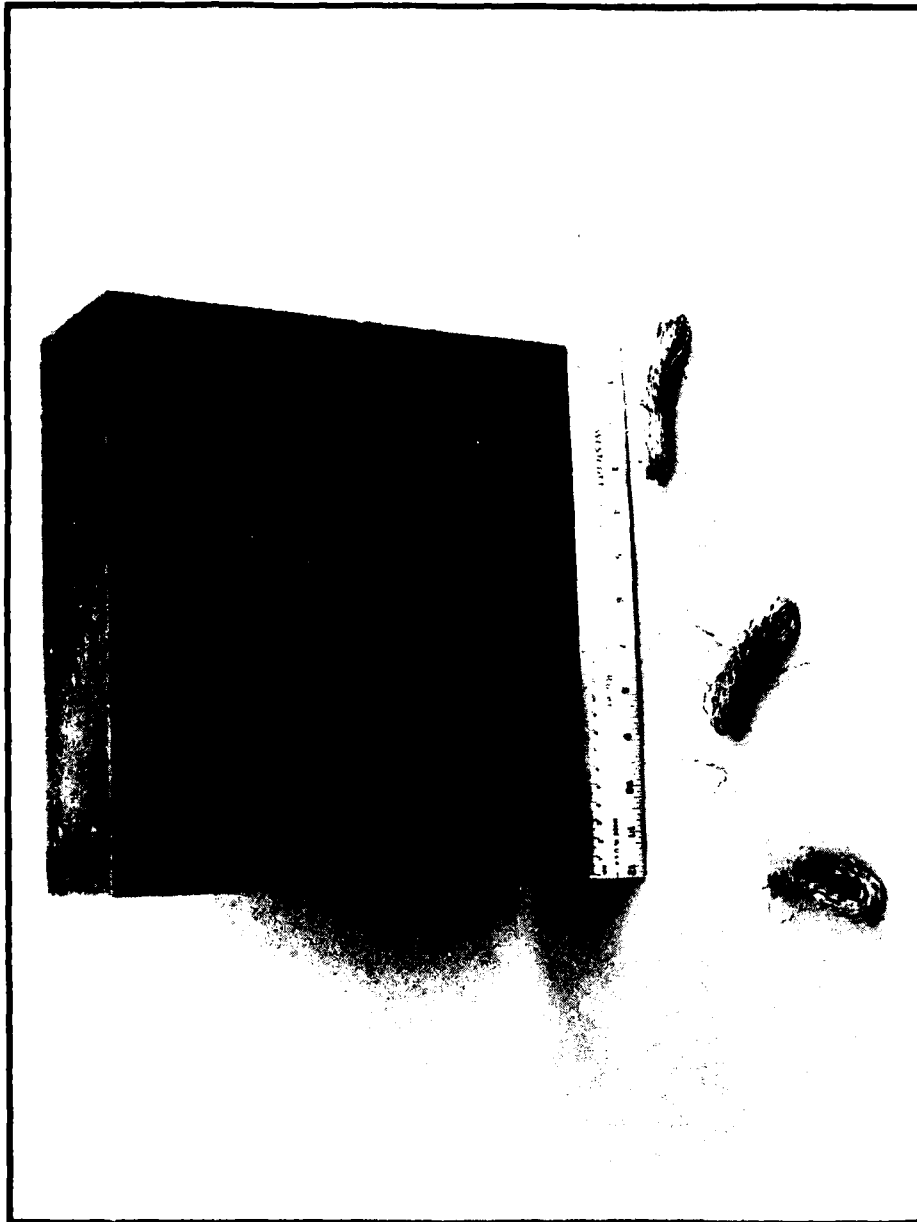


Figure 1
CAST TNT BLOCK USED IN CONSTRUCTION OF
LARGE-SCALE TNT CHARGES AT DRES

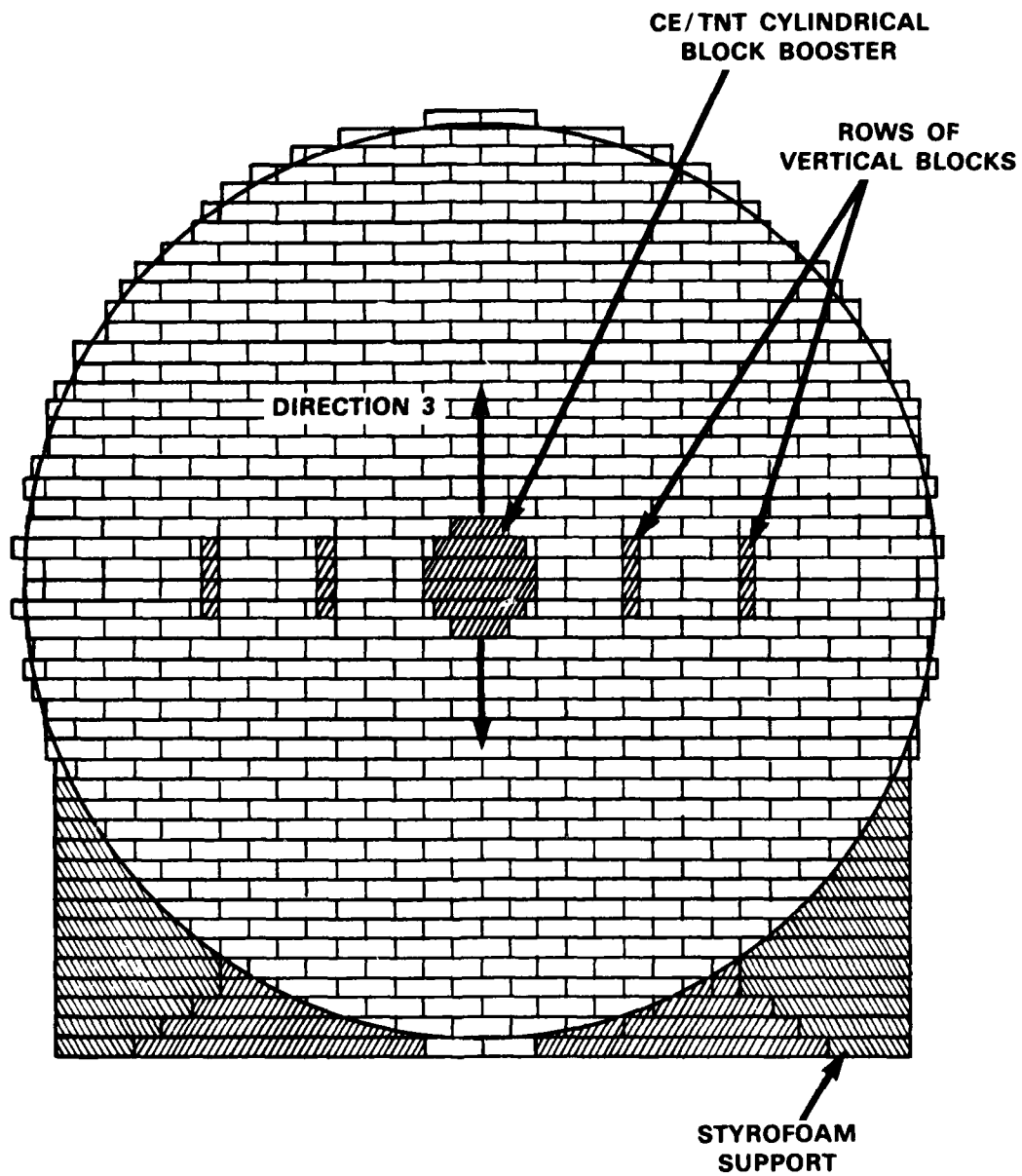


Figure 2

SIDE VIEW, CENTRE SECTION THROUGH 100 TON TNT CHARGE

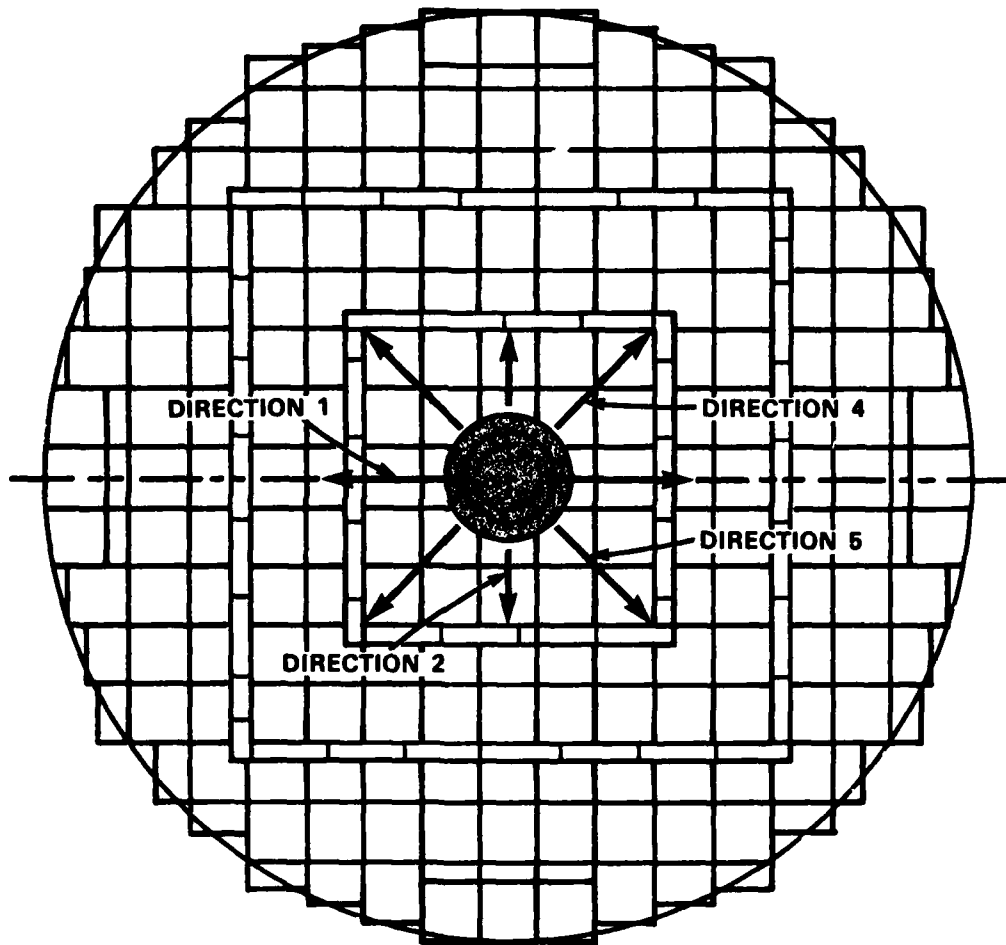
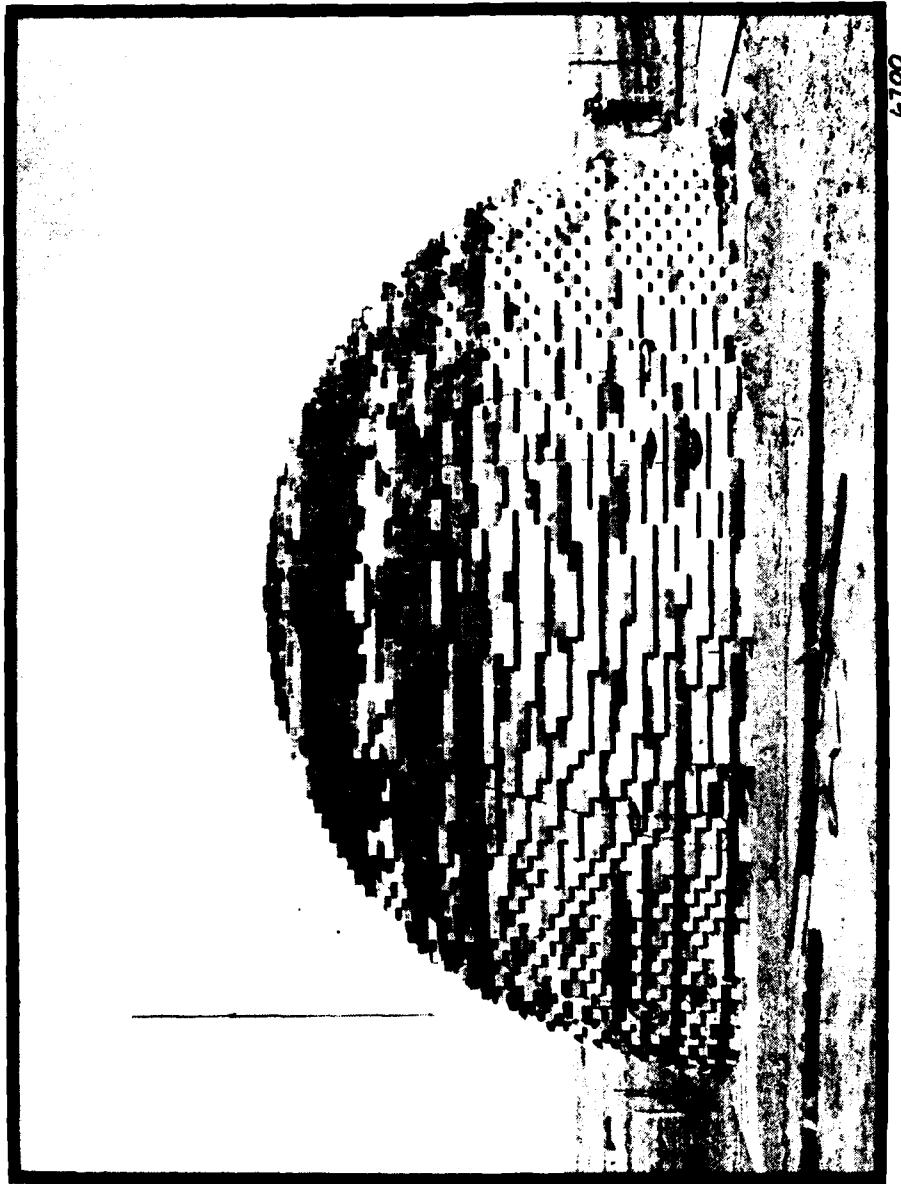


Figure 3
TOP VIEW, CENTRE SECTION THROUGH 100 TON TNT CHARGE

UNCLASSIFIED

SR 385



6700

Figure 4
SIDE VIEW OF STACKED 500 TON TNT HEMISPHERE TANGENT
TO GROUND SURFACE

UNCLASSIFIED

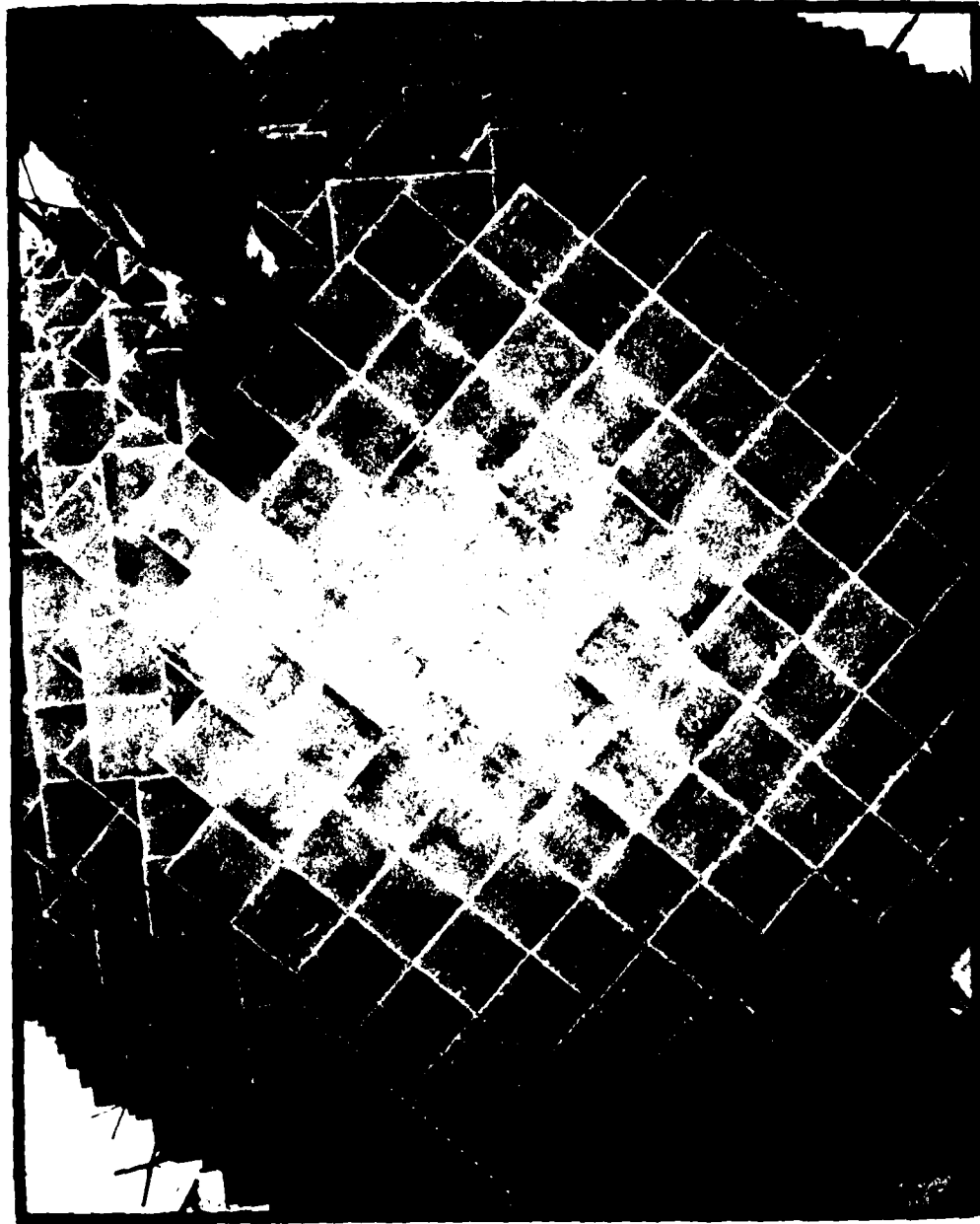


Figure 5

TOP VIEW OF LARGE-SCALE TNT CHARGE, PARTLY CONSTRUCTED
SHOWING ALTERNATE LAYERS ROTATED BY 45°

UNCLASSIFIED

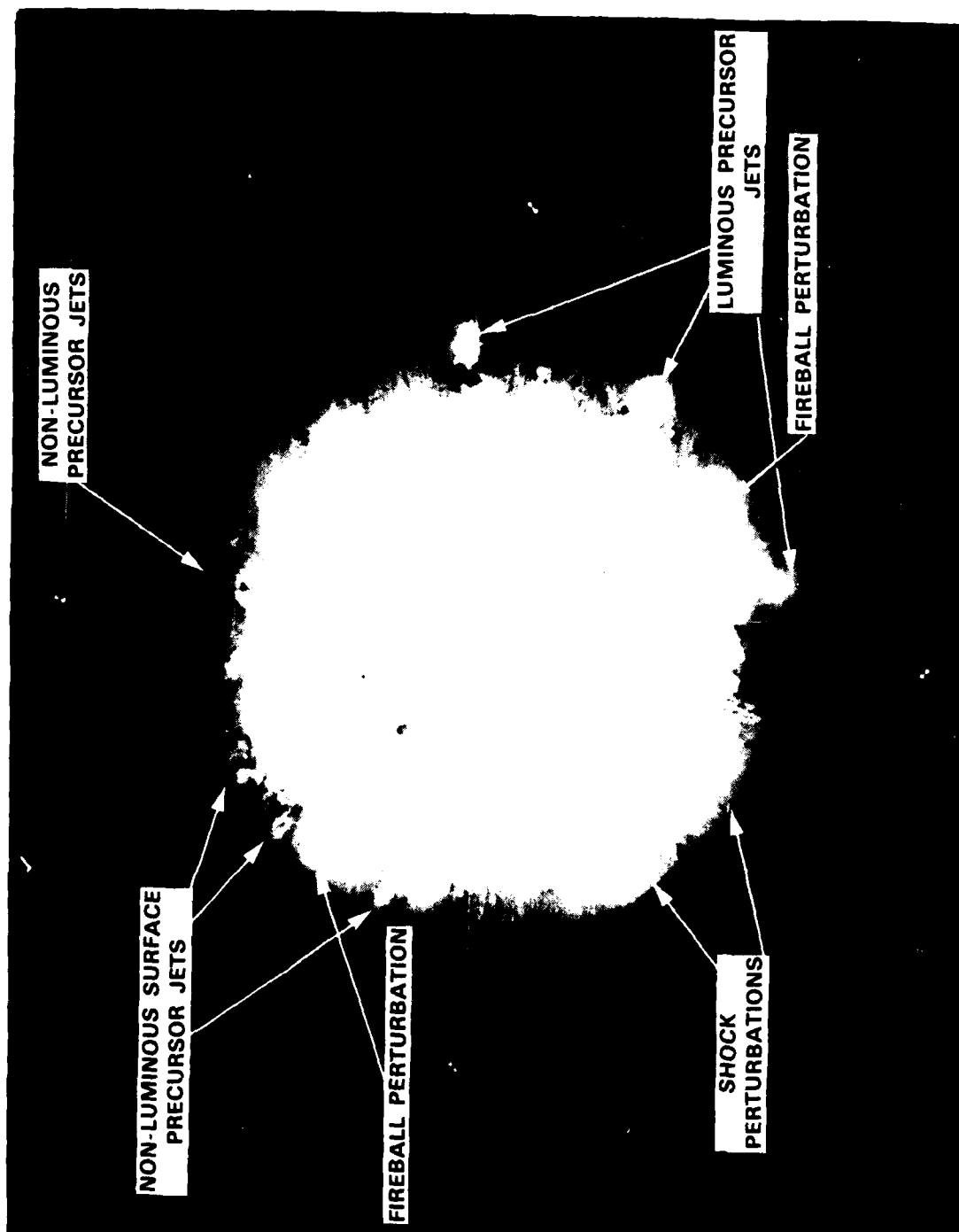
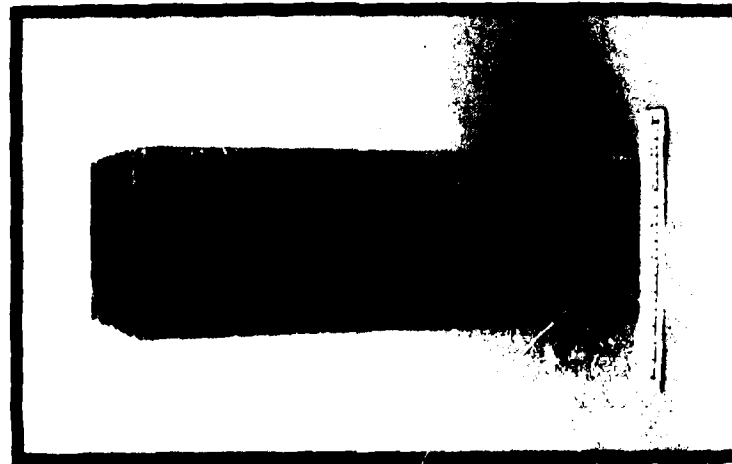
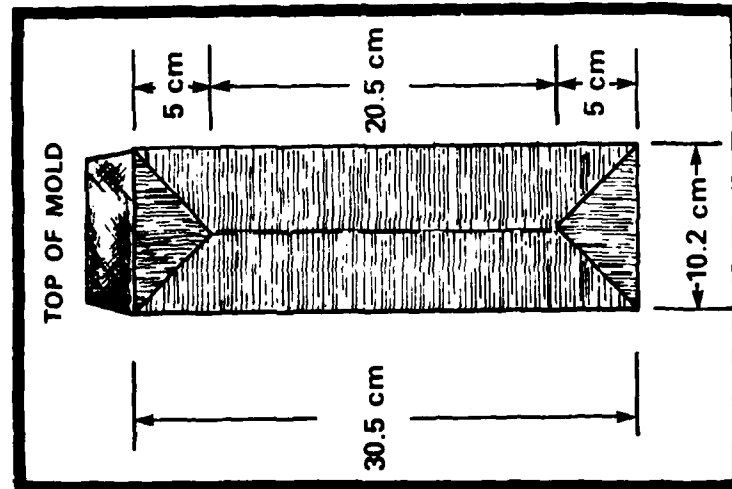


Figure 6

AERIAL VIEW OF DETONATING 500 TON TNT CHARGE
SHOWING ALL TYPES OF ANOMALIES

UNCLASSIFIED

SR 385



9946

Figure 7

CROSS-SECTION THROUGH CENTRE OF TNT BLOCK
REVEALING CRYSTAL STRUCTURE

UNCLASSIFIED



Figure 8

**AERIAL PHOTOGRAPH OF LAYER 13
FROM 500 TON CHARGE (PRAIRIE FLAT)**

UNCLASSIFIED



Figure 9

**EARLY TIME PHOTOGRAPH FROM SPHERICAL 20 TON BLOCK-BUILT
TNT CHARGE SHOWING NON-UNIFORM LIGHT BREAKOUT
AT CHARGE SURFACE**

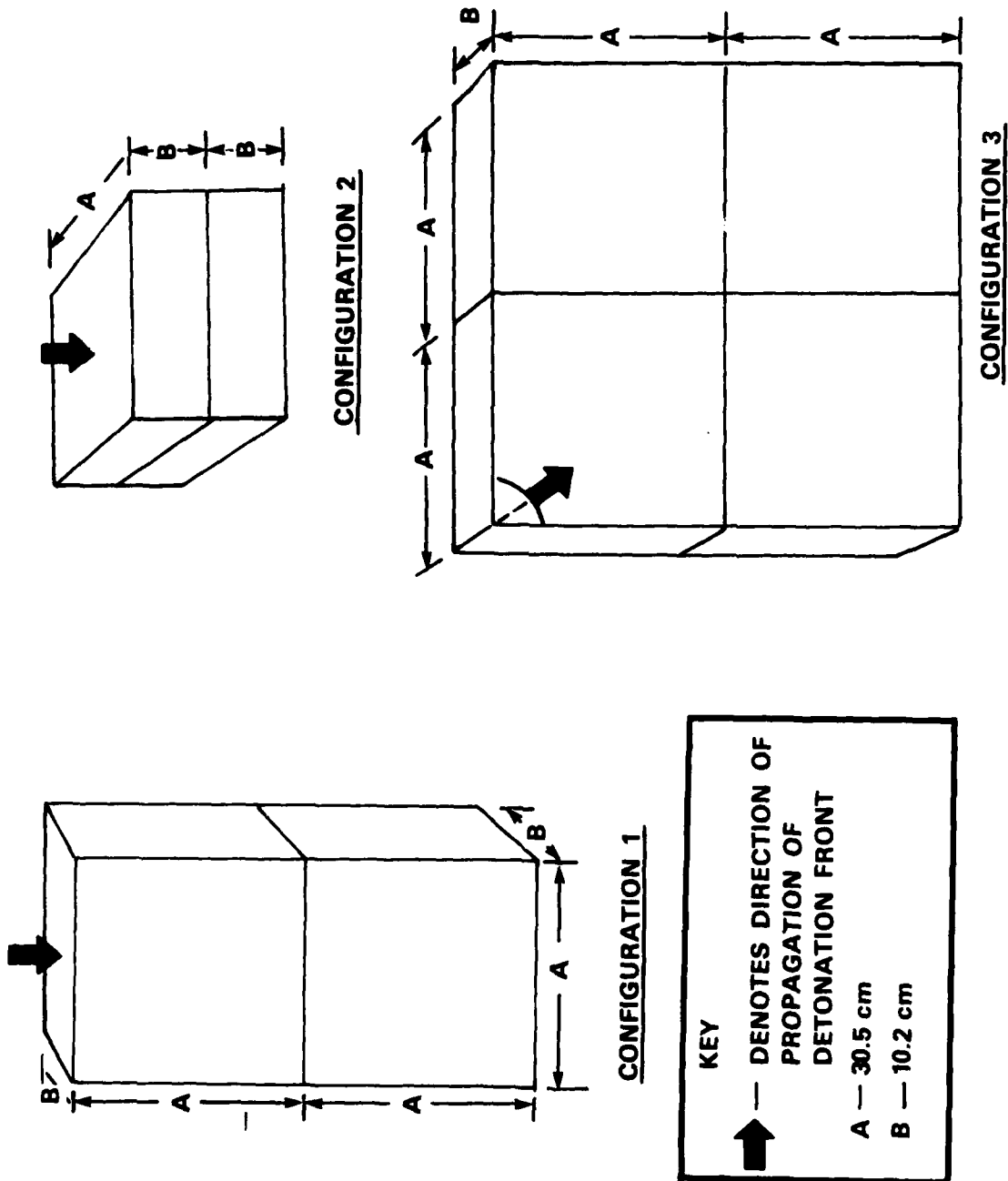


Figure 10
BLOCK CONFIGURATIONS USED IN EXPERIMENTS

UNCLASSIFIED

SR 385

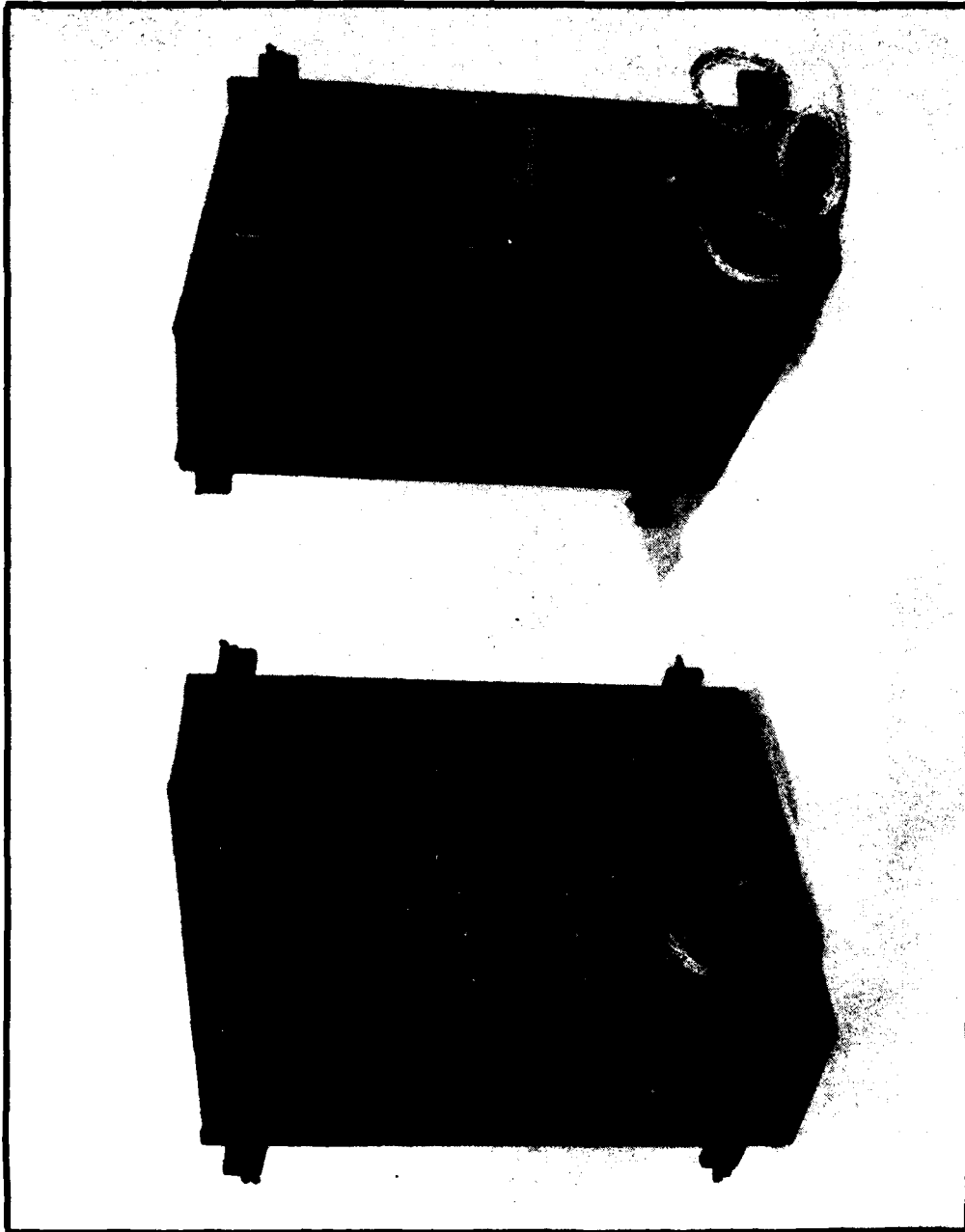


Figure 11
PHOTOGRAPH OF TNT MOLD

UNCLASSIFIED

UNCLASSIFIED

SR 385

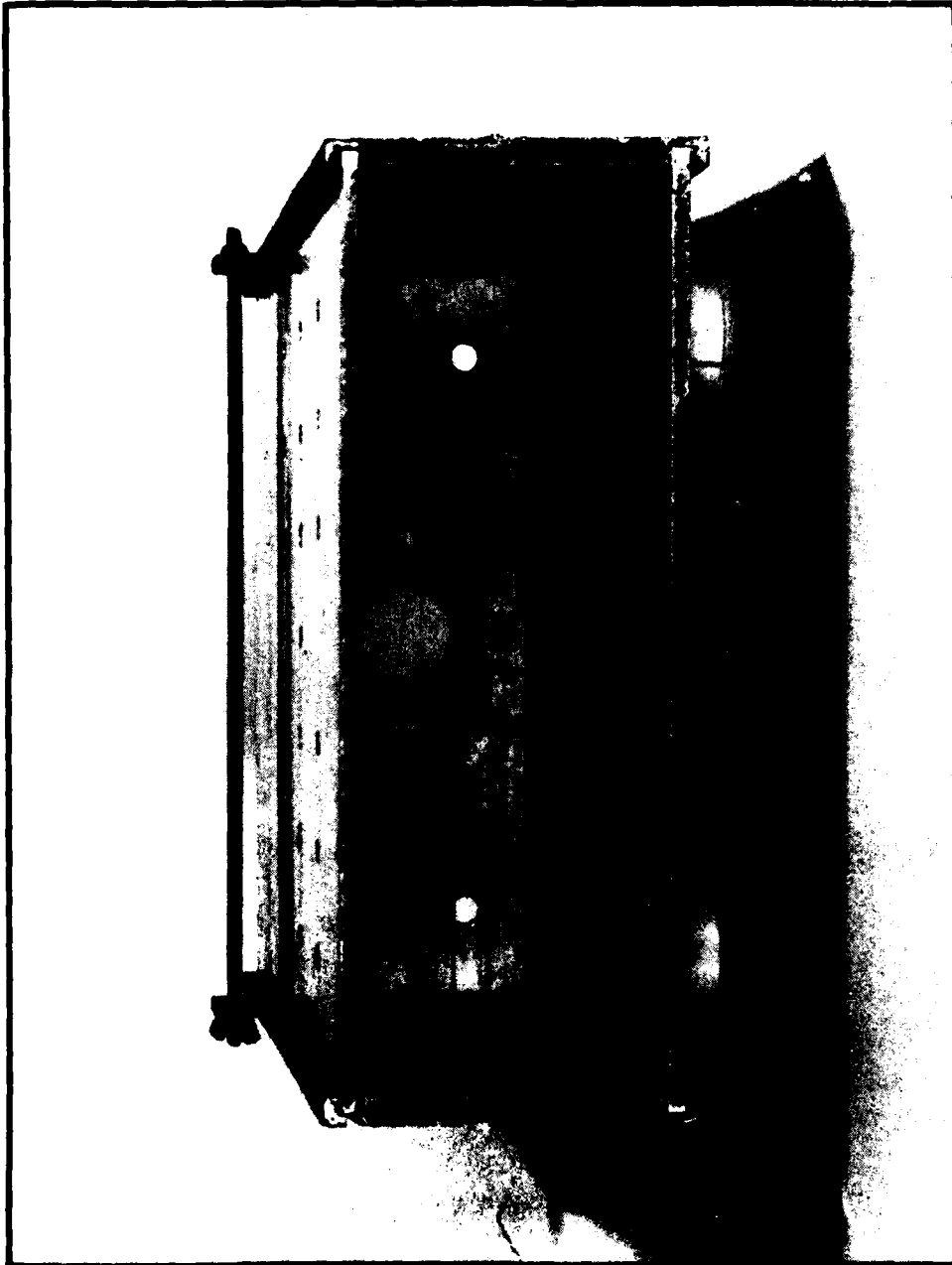


Figure 12
PHOTOGRAPH OF MOLD WITH BOTTOM REMOVED SHOWING DETONATION
VELOCITY PROBES SUSPENDED IN MOLD READY FOR CASTING

UNCLASSIFIED

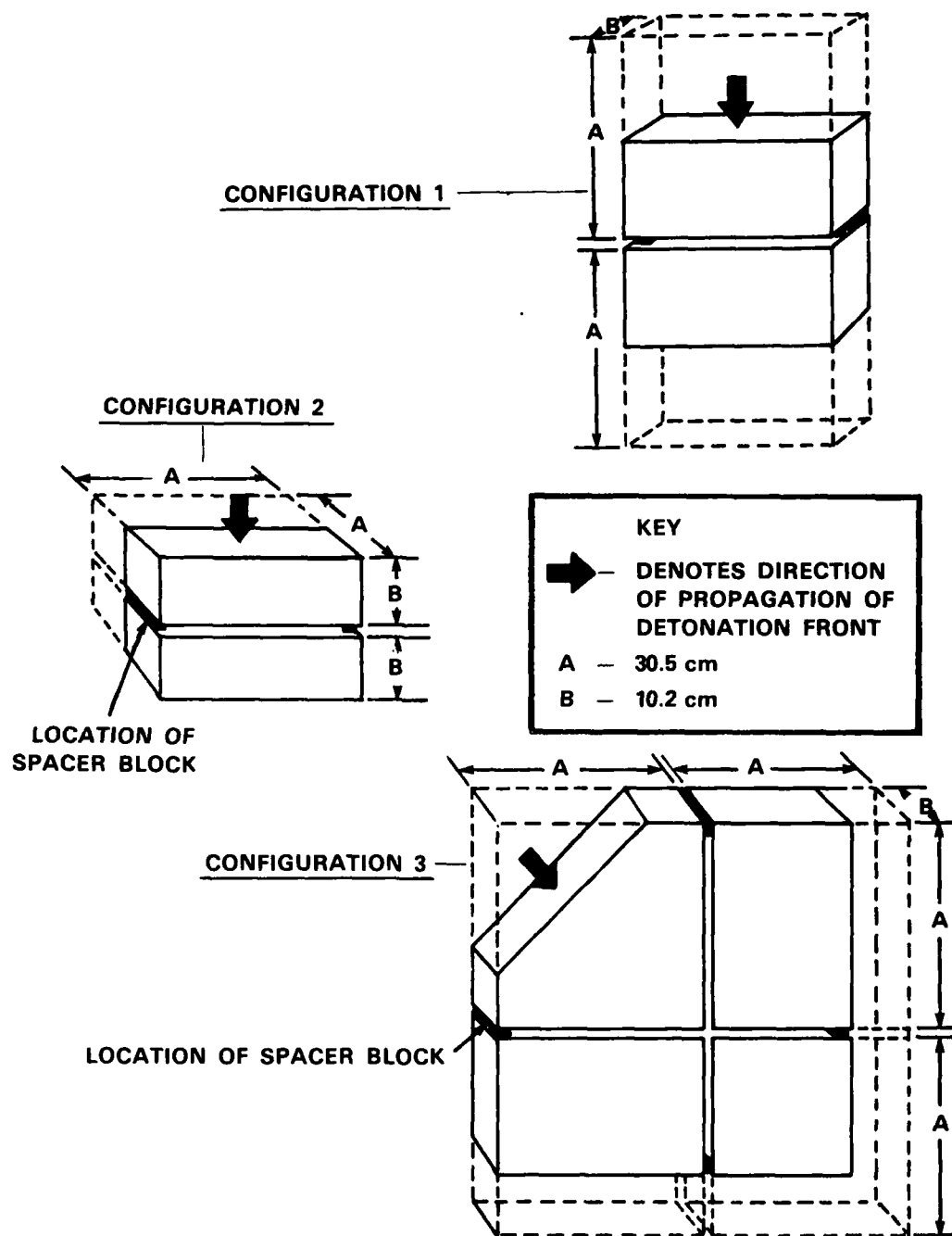


Figure 13

PORTIONS OF TNT BLOCKS FROM CONFIGURATIONS 1 - 3
USED IN EXPERIMENTS

UNCLASSIFIED

SR 385

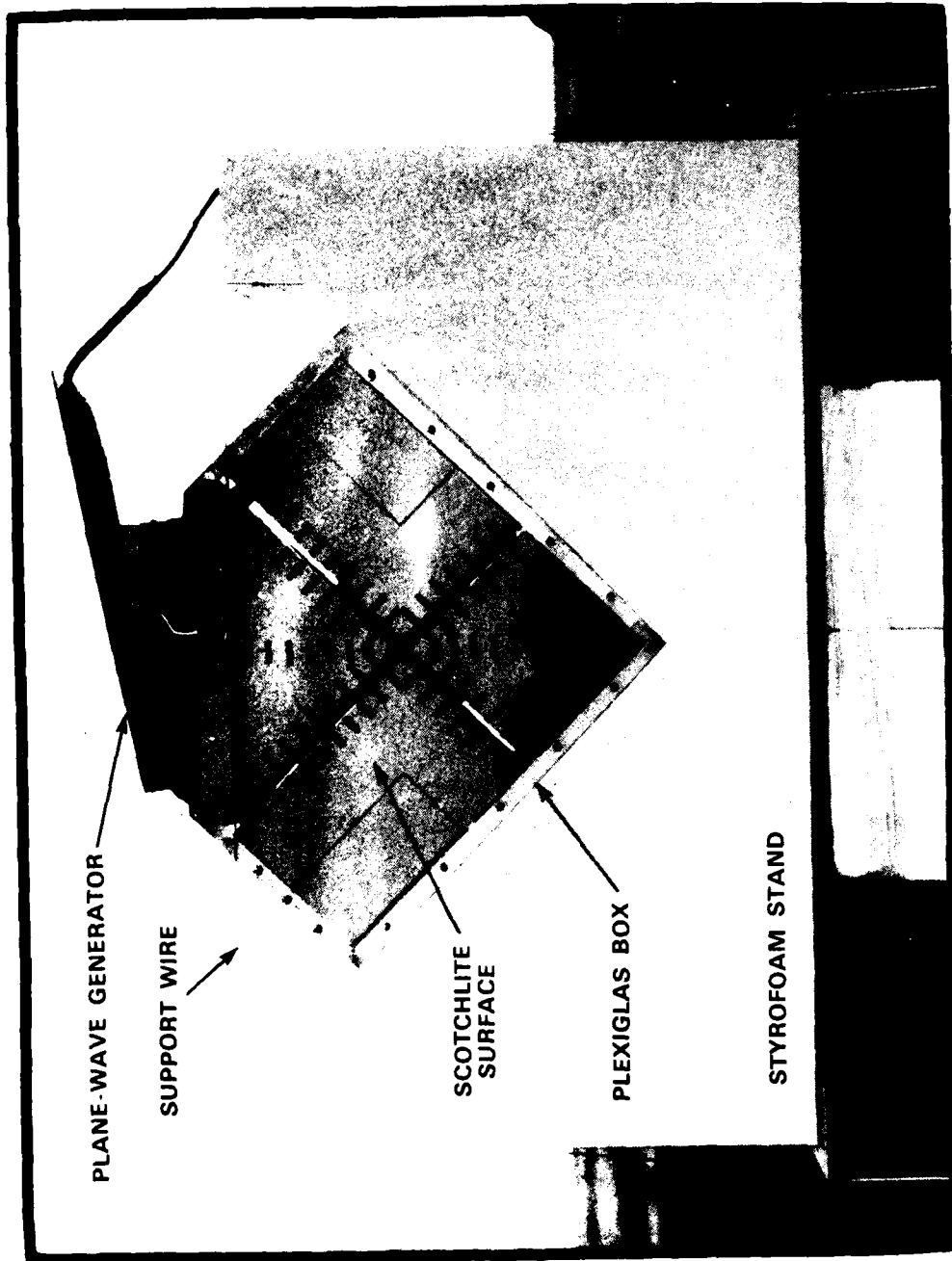


Figure 14
CUTTING OF TNT BLOCK USING STEAM KNIFE

UNCLASSIFIED

UNCLASSIFIED

SR 385



UNCLASSIFIED

Figure 15
PHOTOGRAPH OF FOUR-BLOCK EXPERIMENT (CONFIGURATION 3)
READY FOR FIRING

UNCLASSIFIED

SR 385

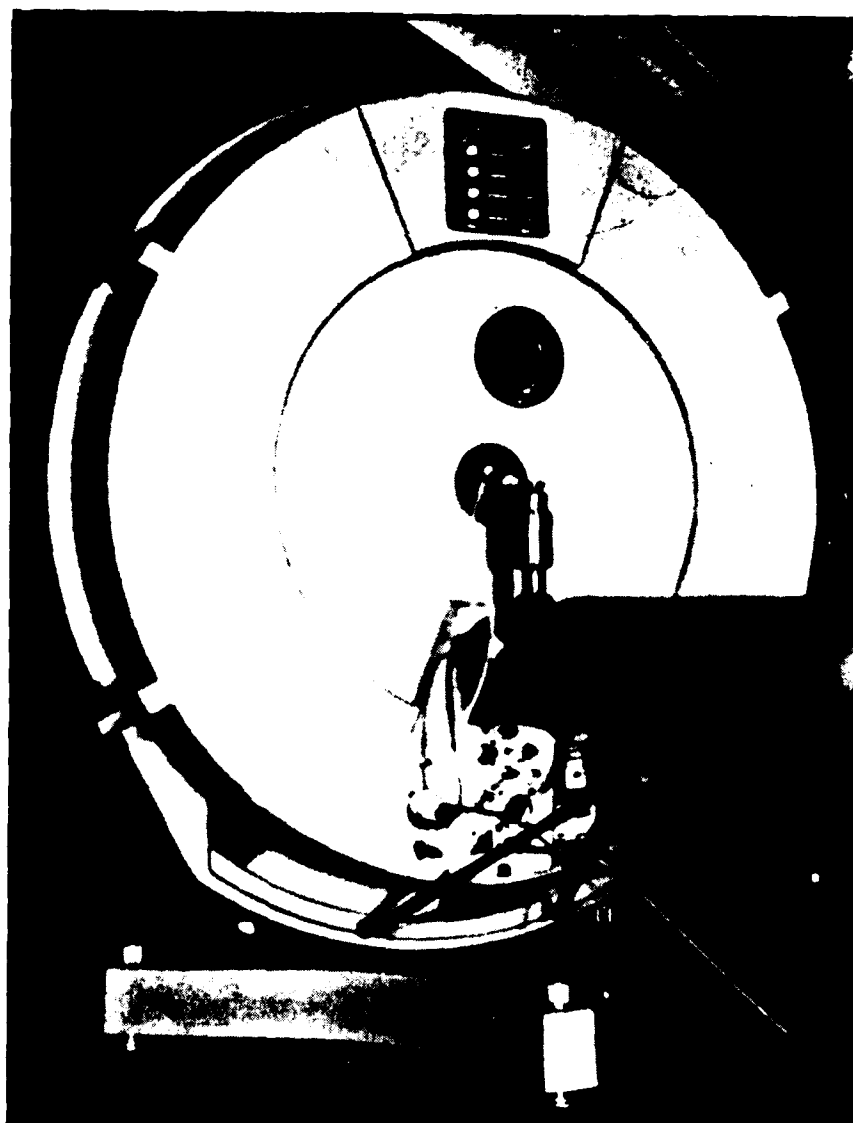


Figure 16

CORDIN MODEL 330A CAMERA

UNCLASSIFIED

UNCLASSIFIED

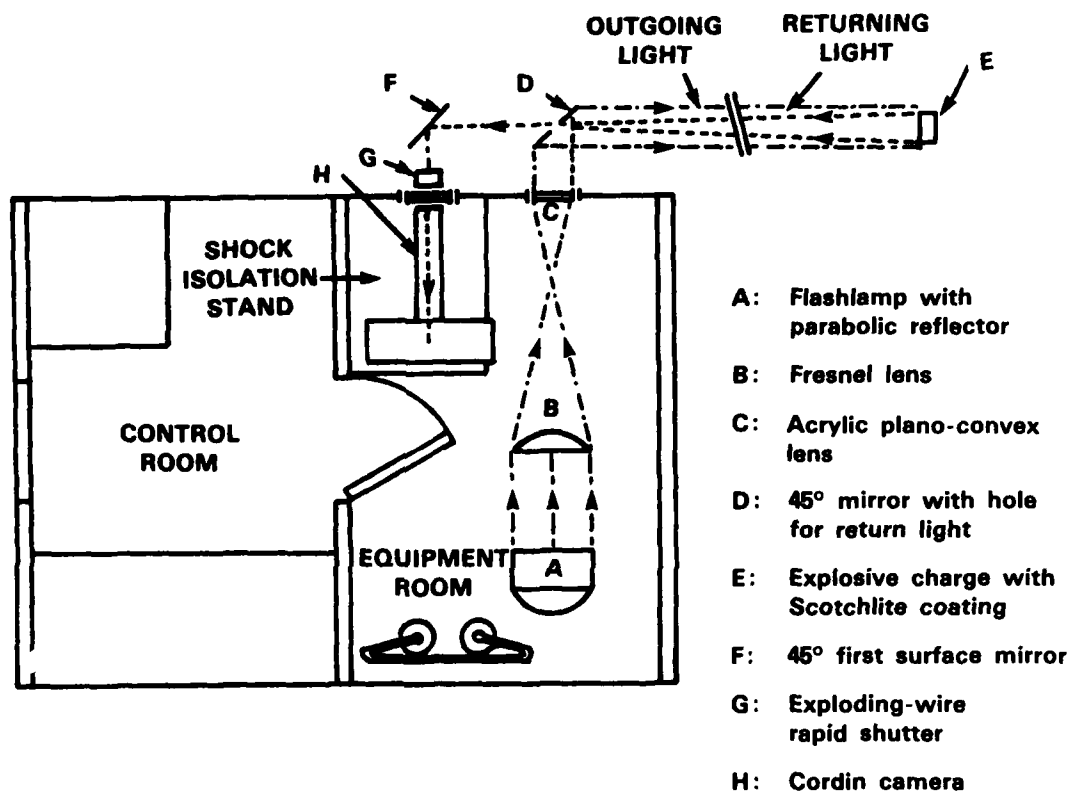
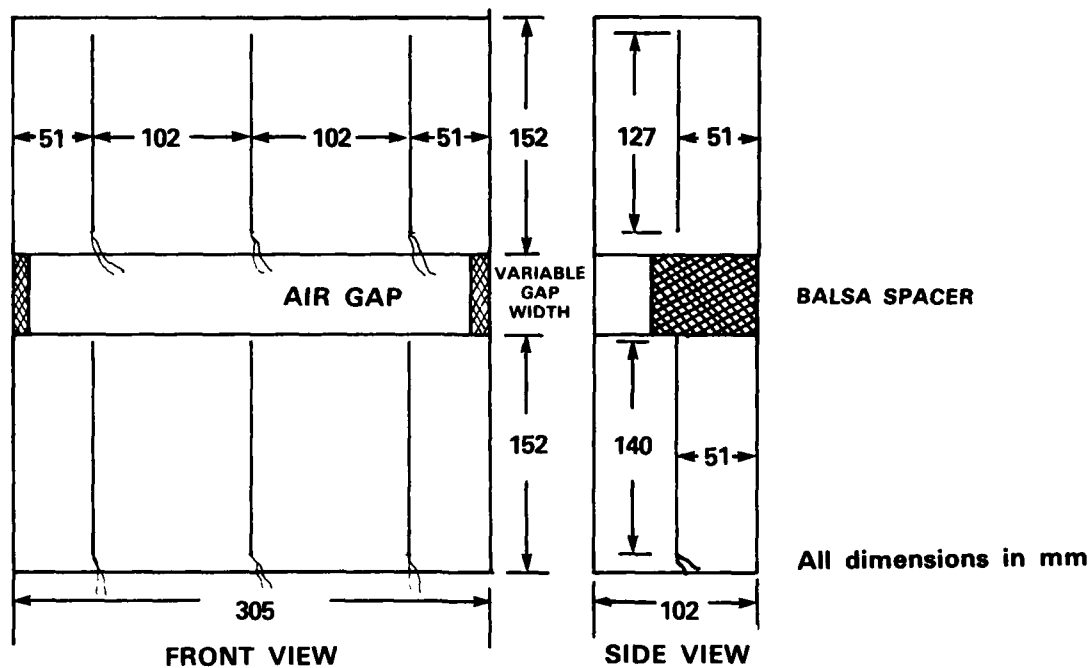


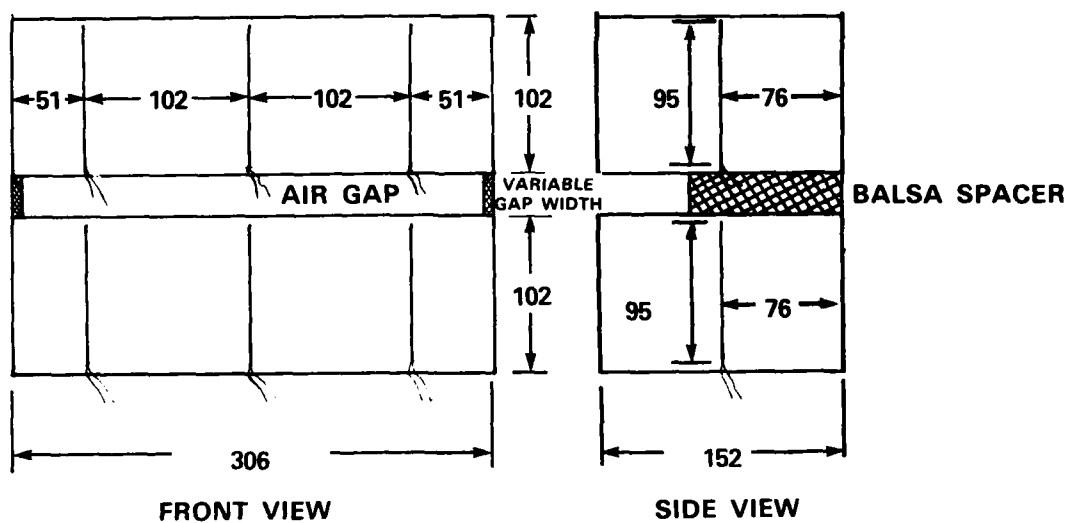
Figure 17

PLAN VIEW OF EXPERIMENTAL LAYOUT SHOWING MIRROR
ARRANGEMENT FOR CAMERA OPTICS

UNCLASSIFIED



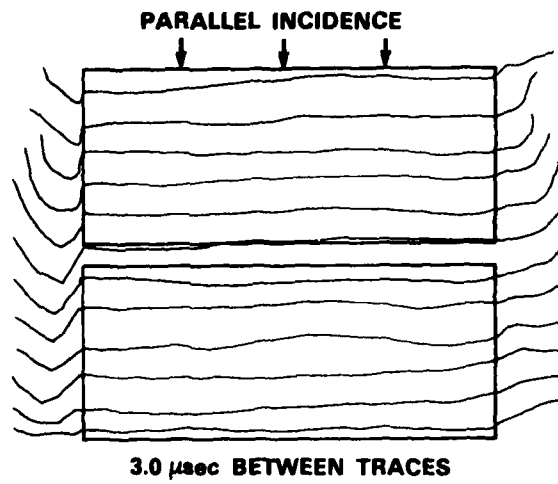
(a) CONFIGURATION 1



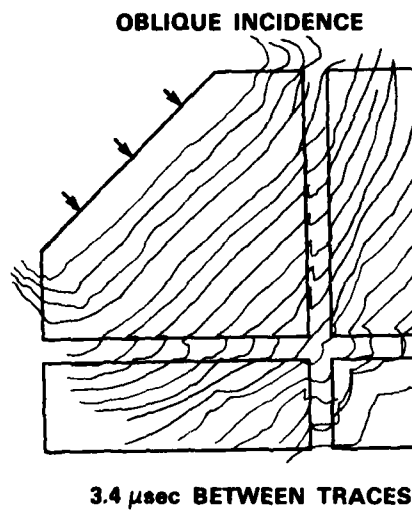
(b) CONFIGURATION 2

Figure 18

POSITIONS OF RESISTIVE PROBES IN TNT BLOCKS



(a) 2-BLOCK CONFIGURATION



(b) 4-BLOCK CONFIGURATION

Figure 19
COMPOSITE DRAWING FROM FRAMING RECORD
UNCLASSIFIED

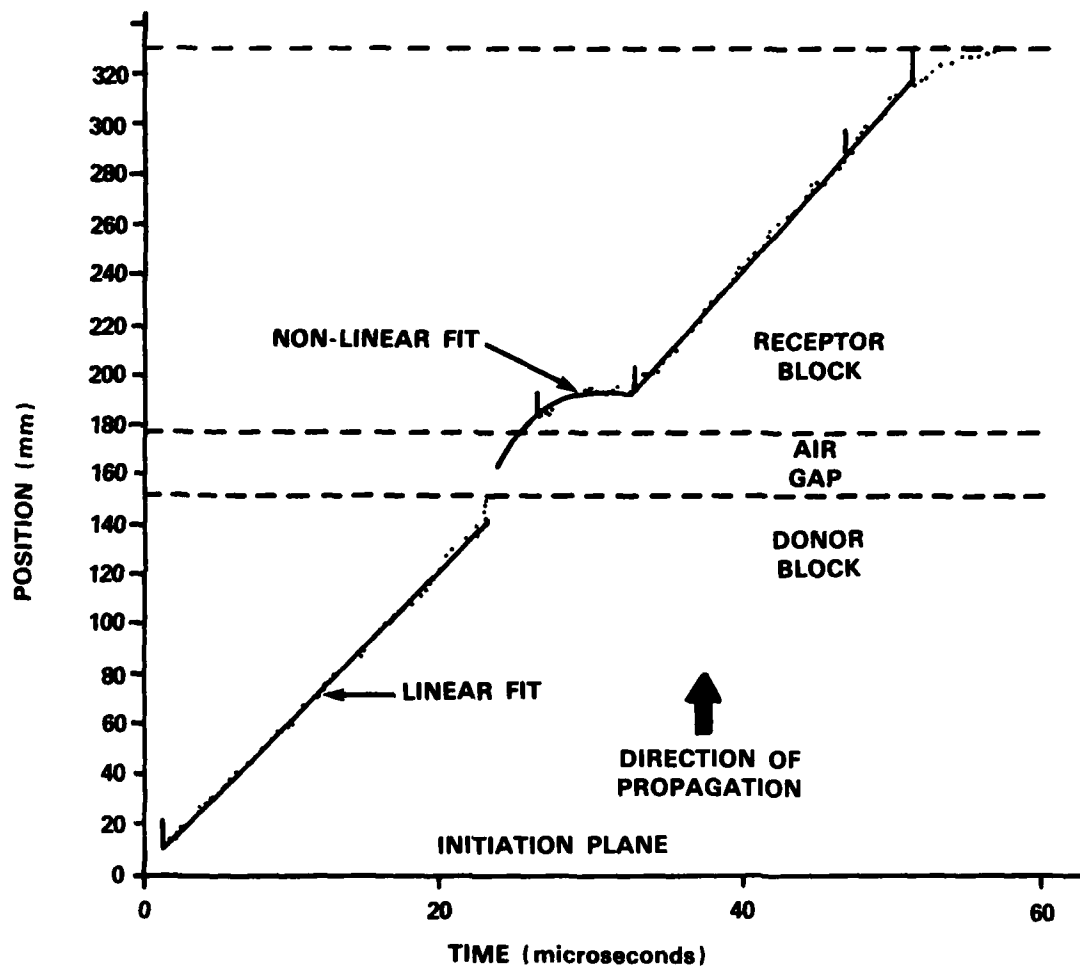


Figure 20

TYPICAL DIGITIZED RECORD FROM STREAK FILM

UNCLASSIFIED

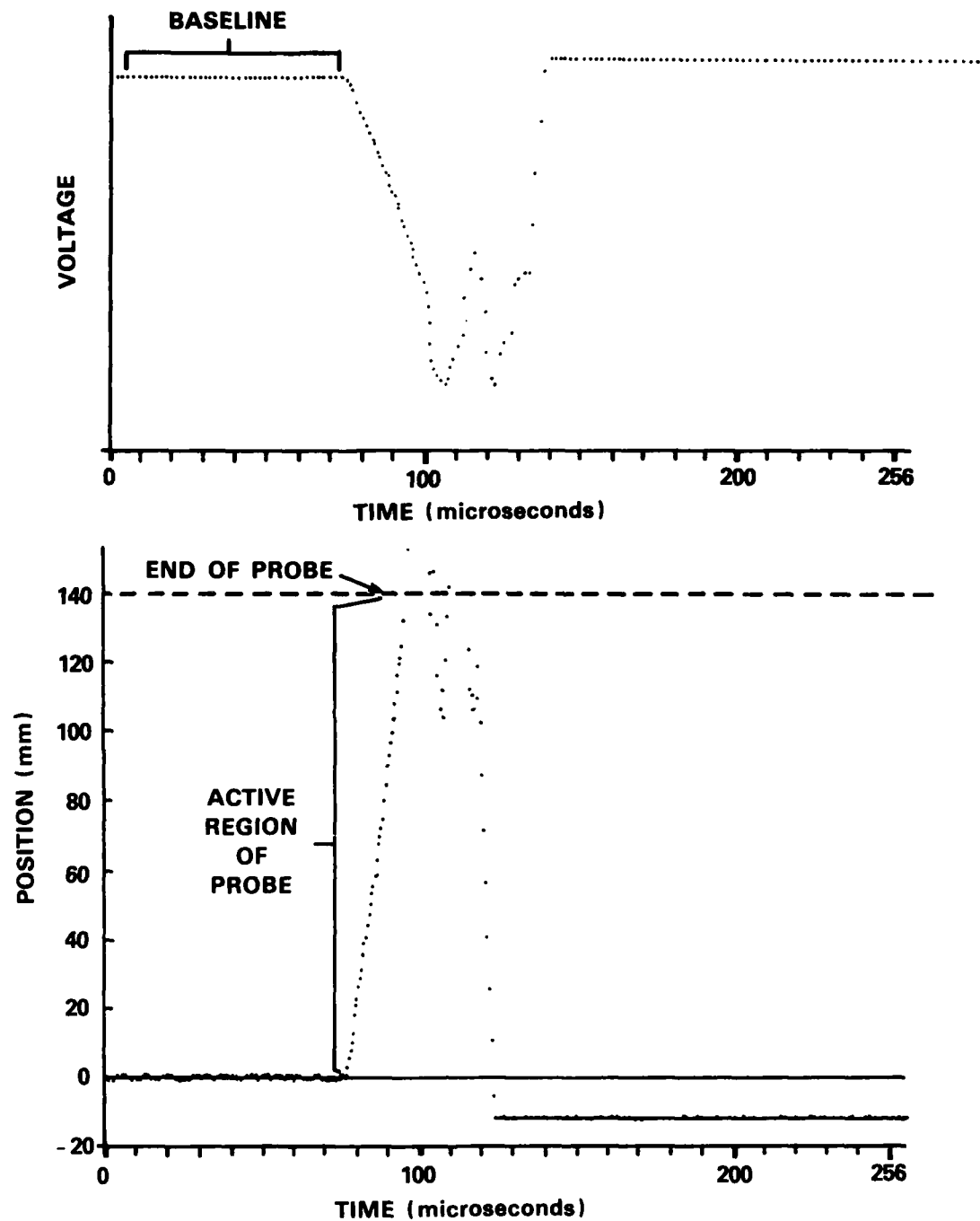


Figure 21

TYPICAL DIGITIZED RECORDS FROM RESISTIVE DETONATION
VELOCITY PROBES
UNCLASSIFIED

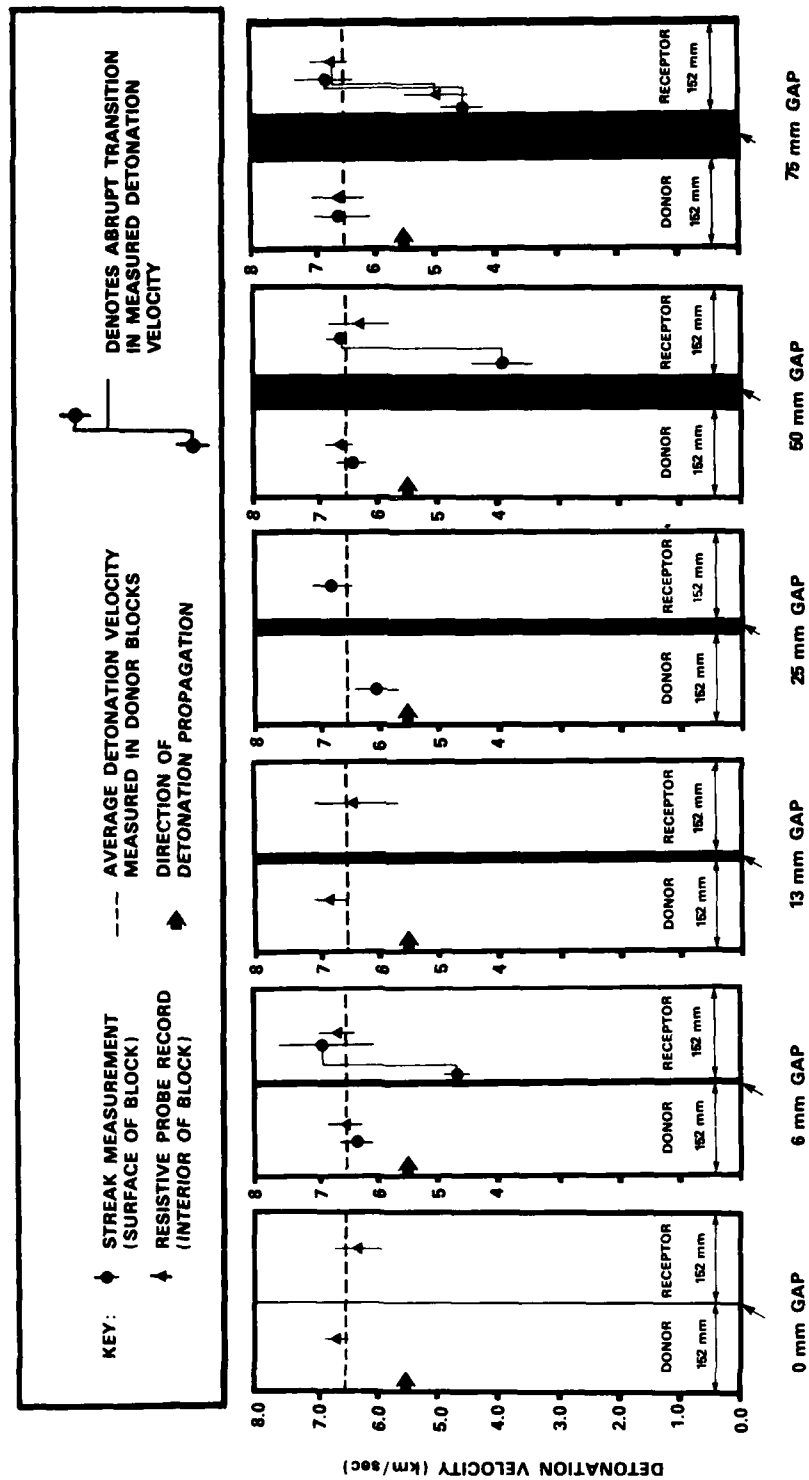


Figure 22
 DETONATION VELOCITY MEASUREMENTS FROM CONFIGURATION 1
 EXPERIMENTS (UNCONFINED BLOCKS)

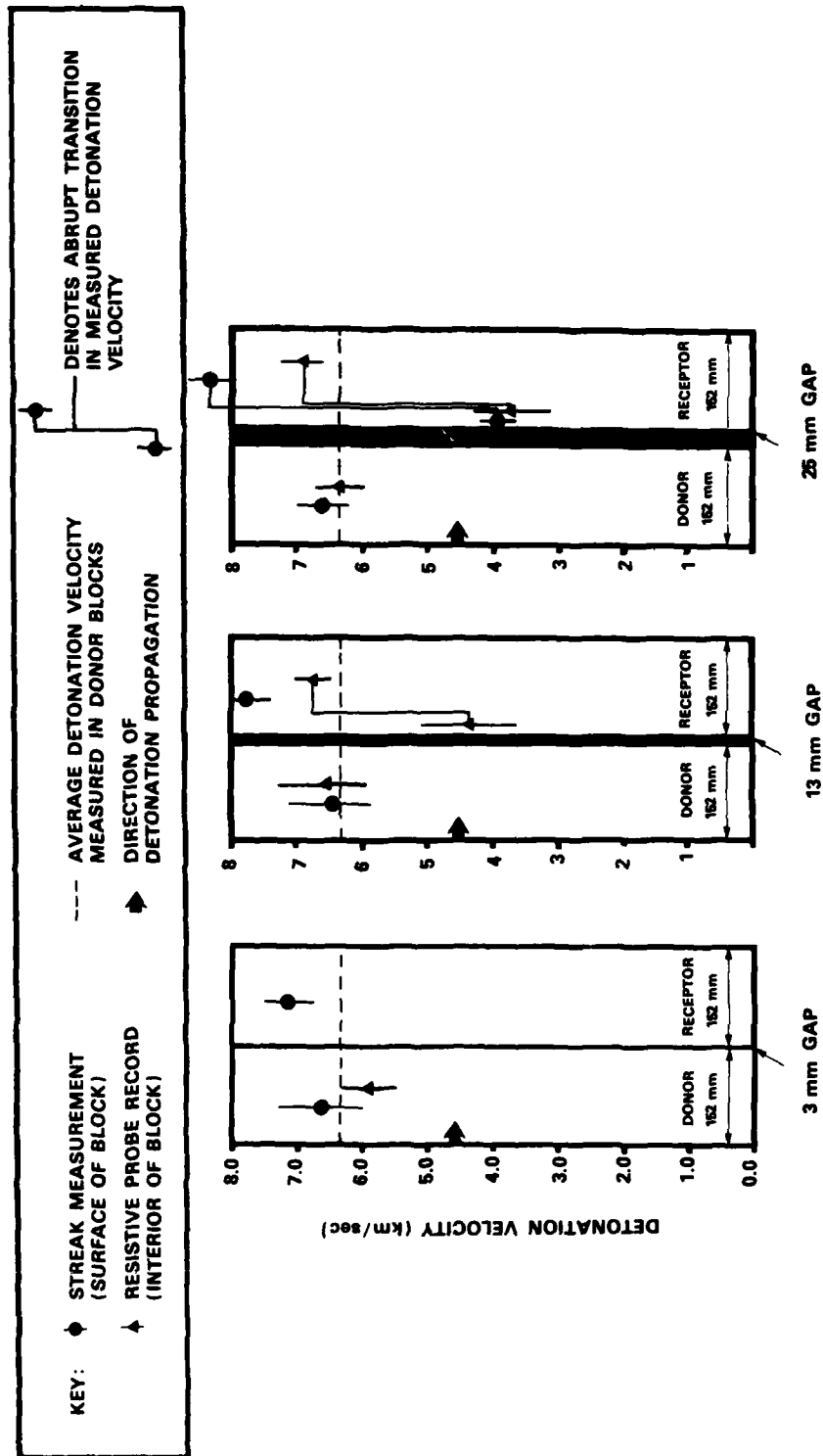


Figure 23

DETONATION VELOCITY MEASUREMENTS FROM CONFIGURATION 1
EXPERIMENTS (CONFINED BLOCKS)

UNCLASSIFIED

SR 385

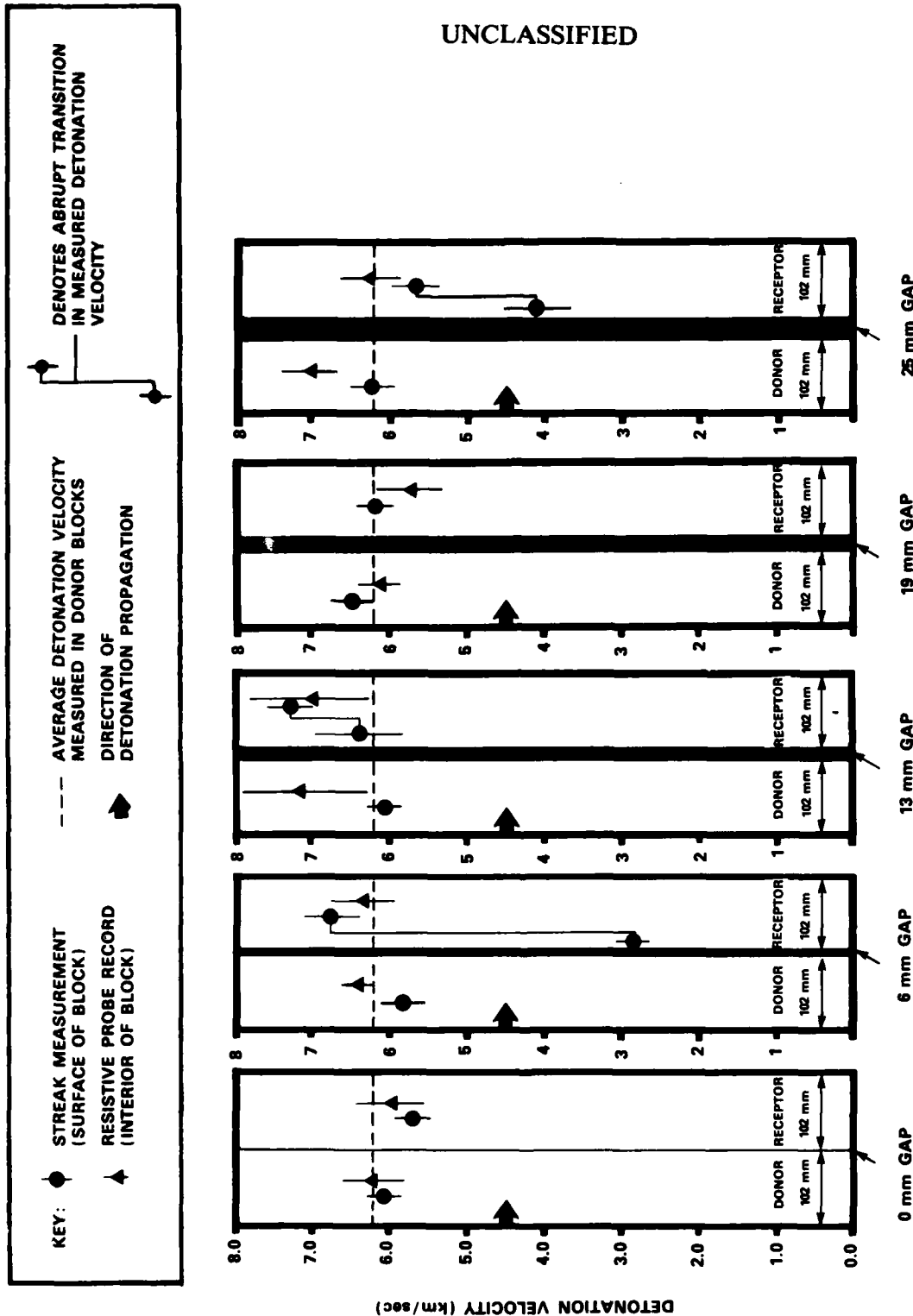
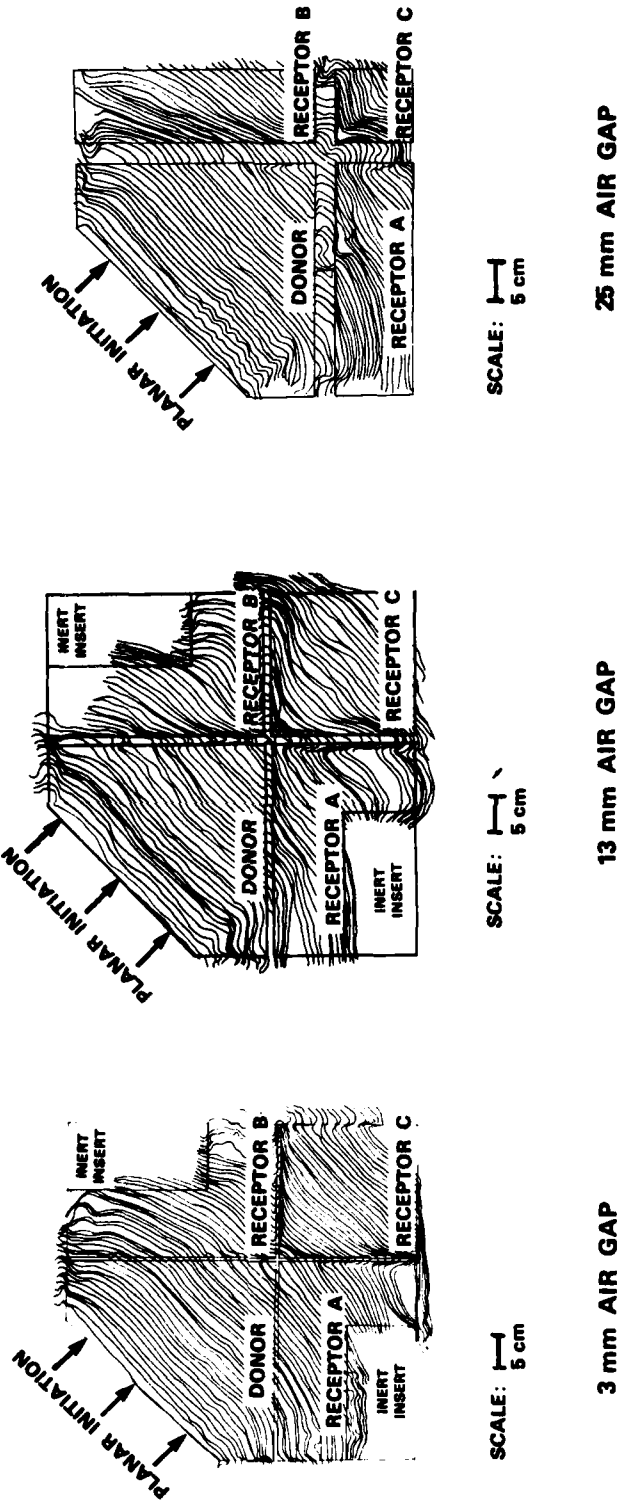


Figure 24
DETONATION VELOCITY MEASUREMENTS FROM CONFIGURATION 2
EXPERIMENTS (UNCONFINED BLOCKS)

UNCLASSIFIED

UNCLASSIFIED

SR 385



UNCLASSIFIED

Figure 25
COMPOSITE TRACINGS FROM FRAMING CAMERA SHOWING PROGRESS
OF DETONATION FRONT ACROSS AIR GAPS
(UNCONFINED TNT BLOCKS)

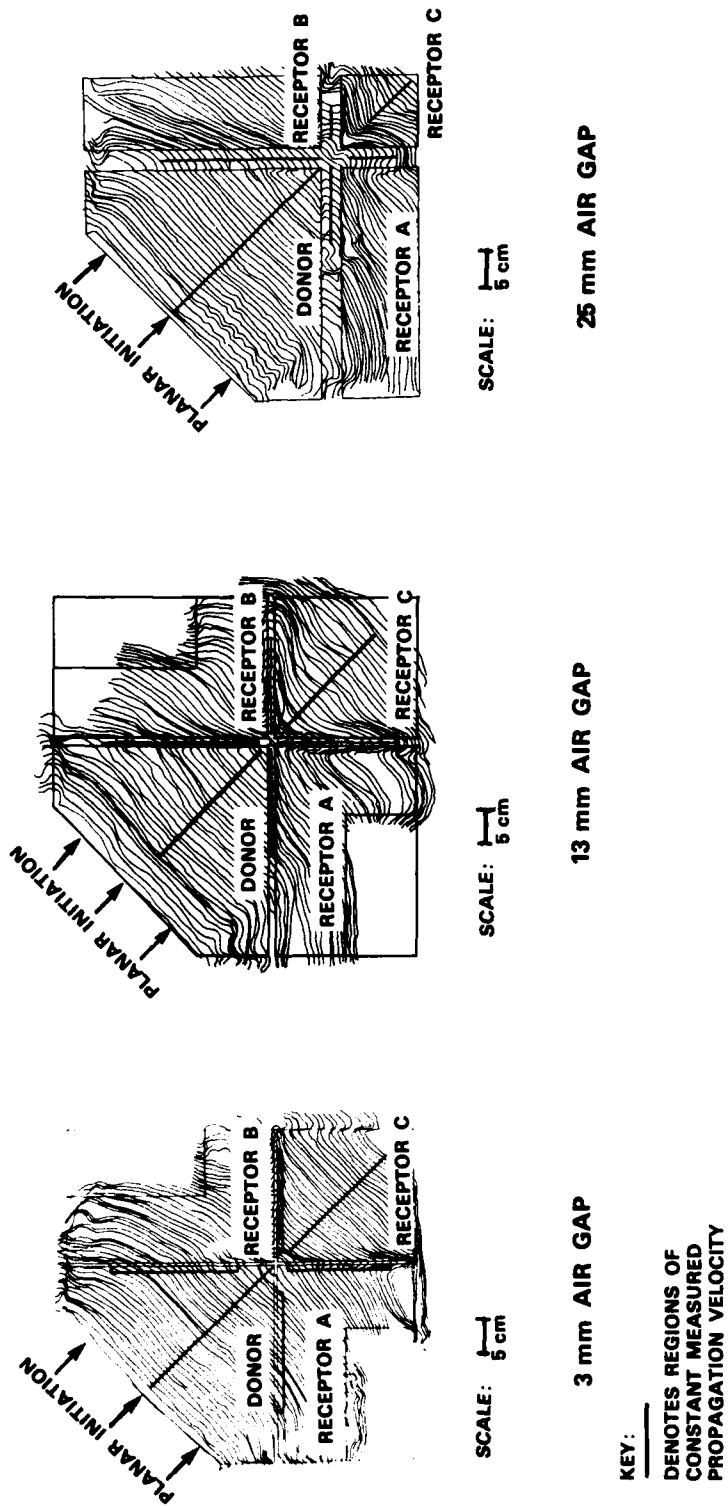


Figure 26
COMPOSITE TRACINGS FROM FRAMING CAMERA SHOWING LINES
OF CONSTANT PROPAGATION VELOCITY
(UNCONFINED TNT BLOCKS)

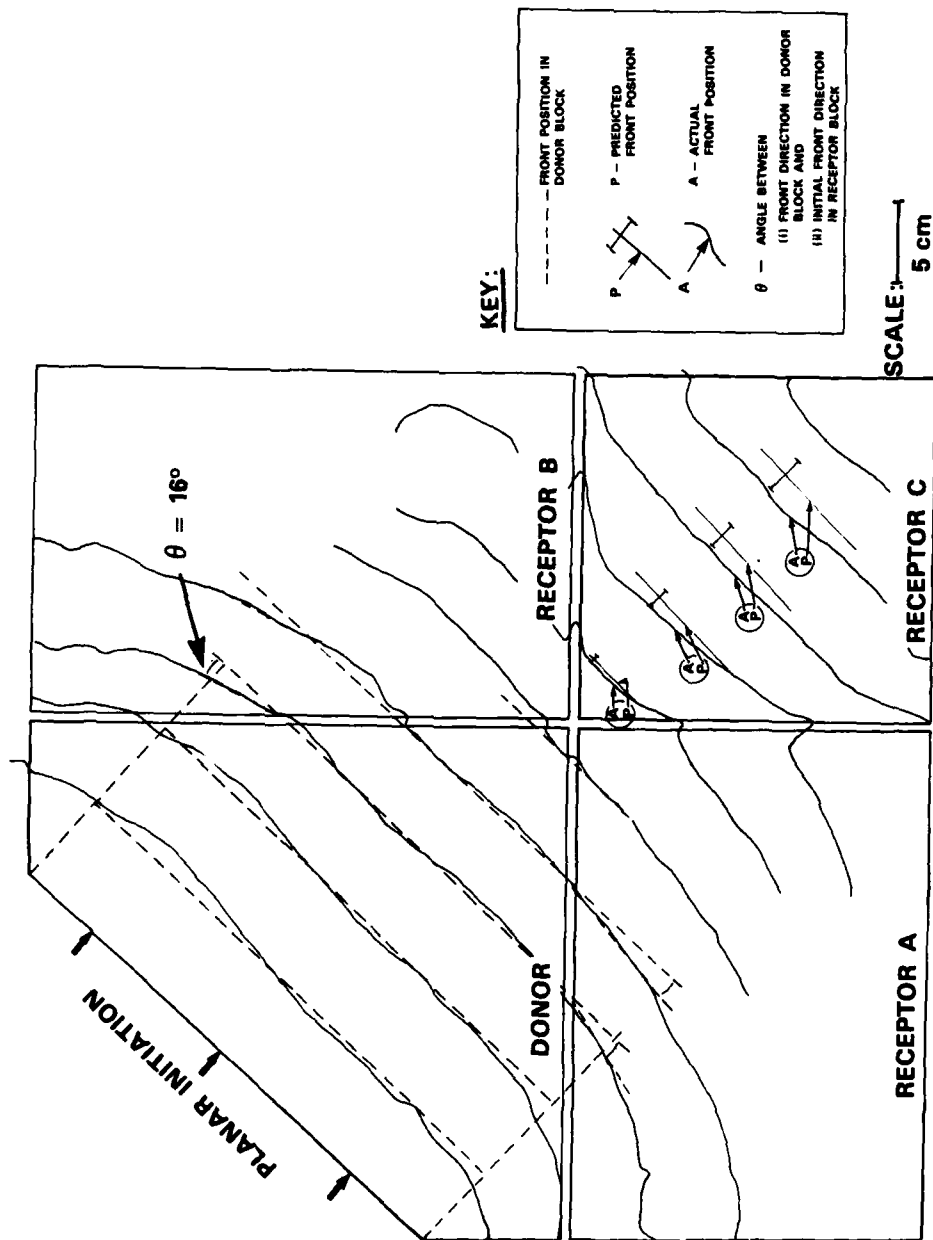


Figure 27

CHANGES IN SHAPE AND POSITION OF DETONATION FRONT IN
RECEPTOR BLOCKS CAUSED BY 3 mm AIR GAP

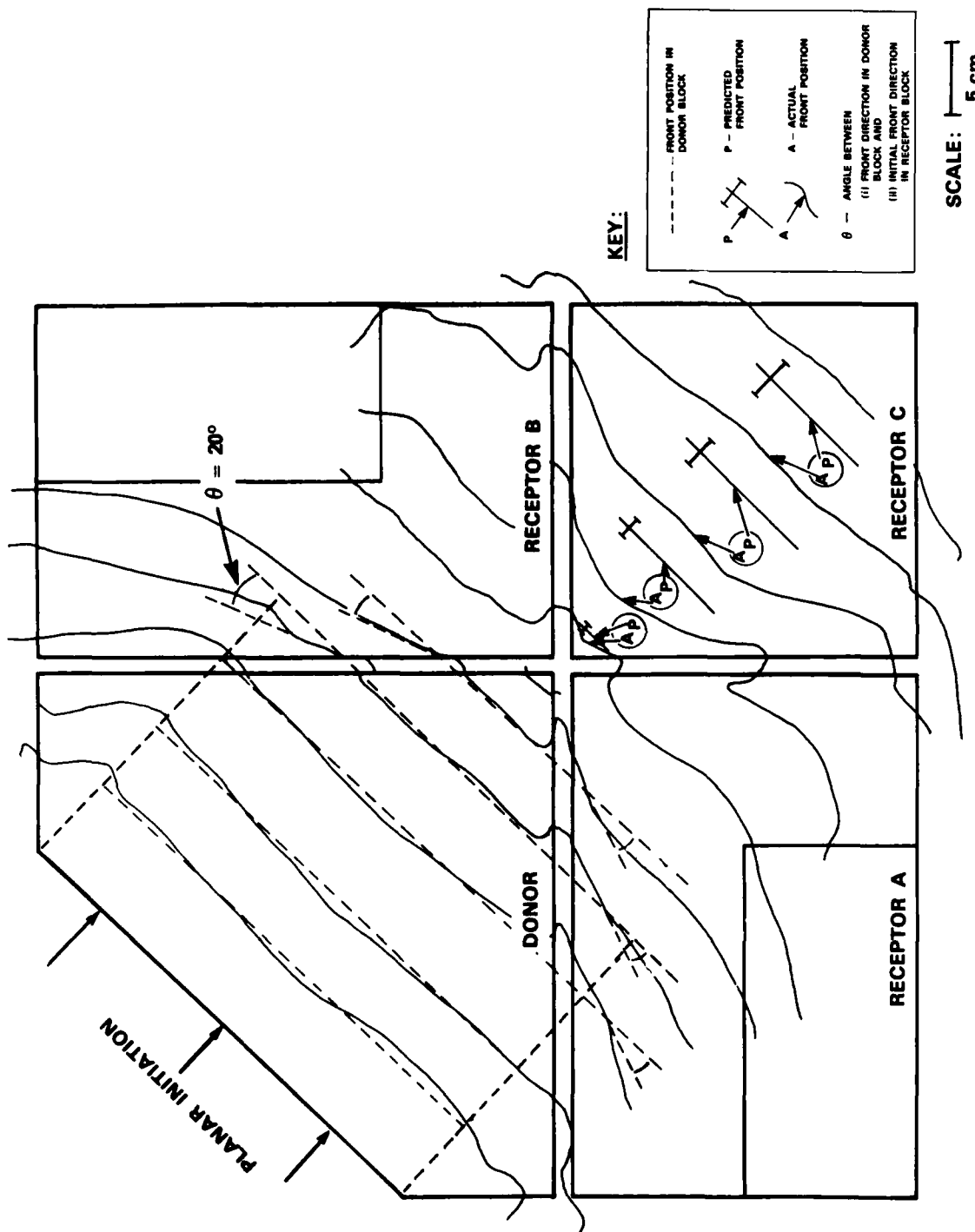


Figure 28

CHANGES IN SHAPE AND POSITION OF DETONATION FRONT IN
RECEPTOR BLOCKS CAUSED BY 13 mm AIR GAP

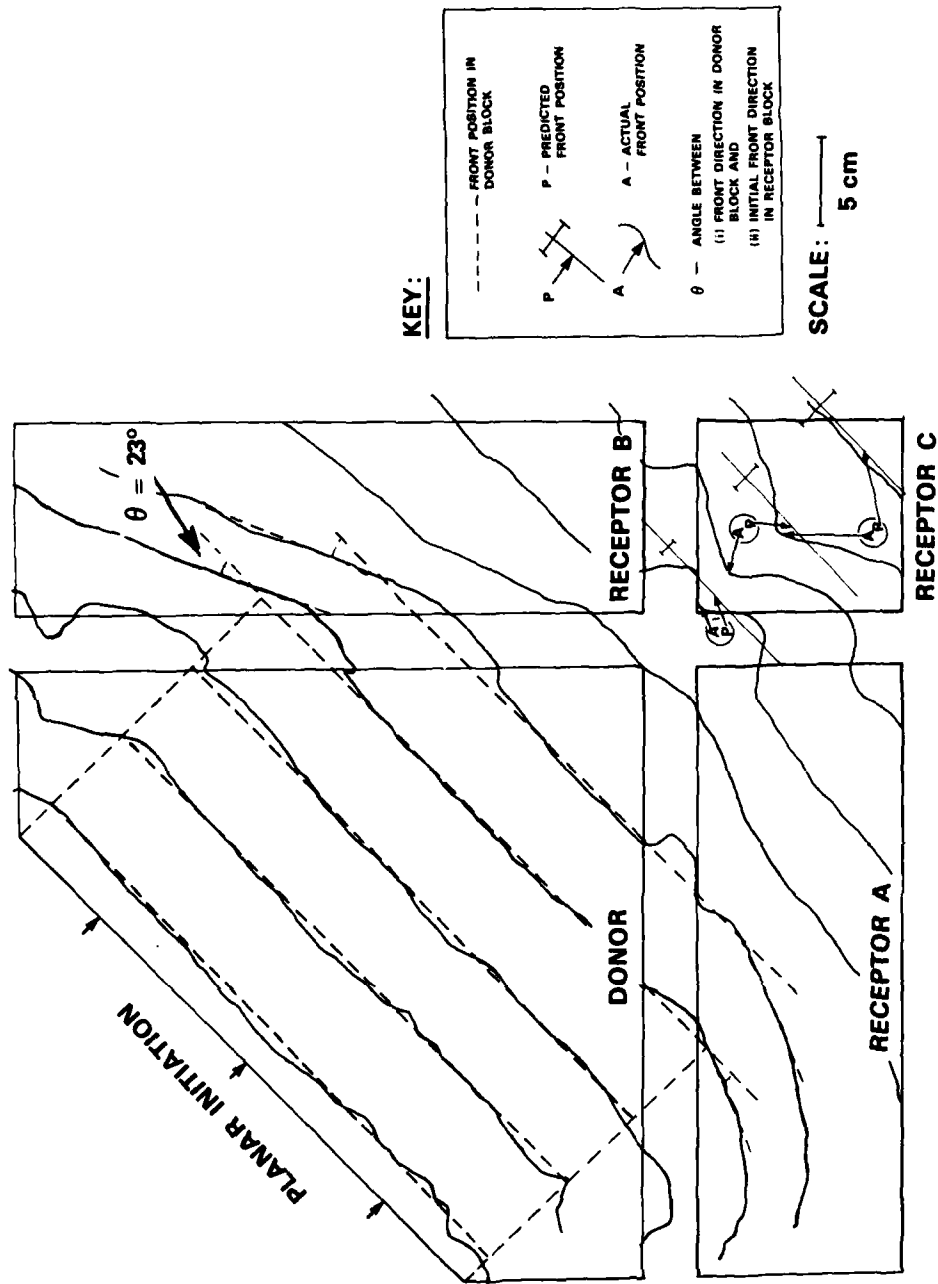
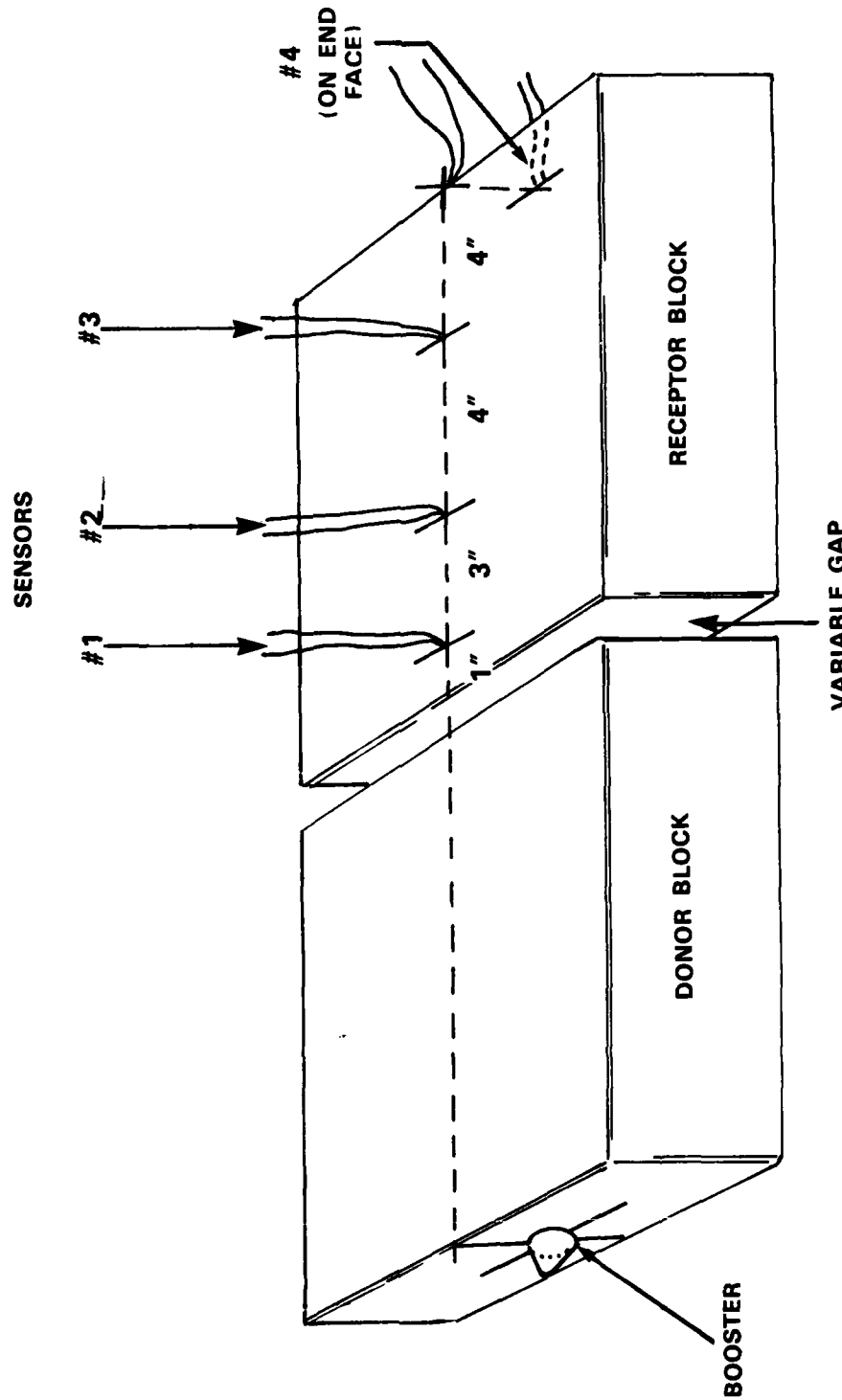


Figure 29

CHANGES IN SHAPE AND POSITION OF DETONATION FRONT IN
RECEPTOR BLOCKS CAUSED BY 25 mm AIR GAP

UNCLASSIFIED

SR 385



UNCLASSIFIED

Figure 30

HOLSGROVE'S EXPERIMENTAL CONFIGURATION (HOLSGROVE, 1968)

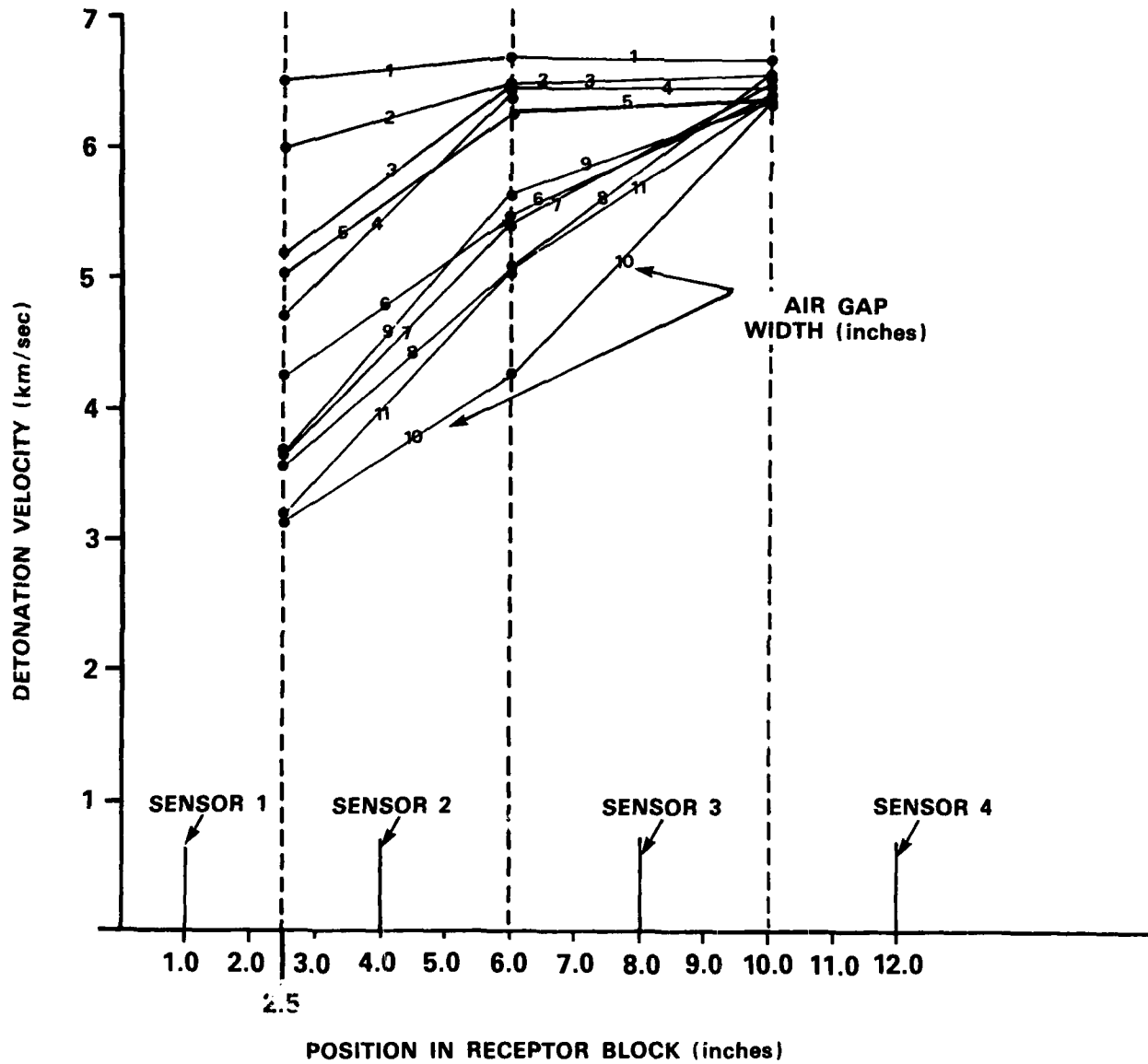


Figure 31

EFFECT OF AIR GAP WIDTH ON DETONATION VELOCITY IN
RECEPTOR BLOCK (HOLSGROVE, 1968)

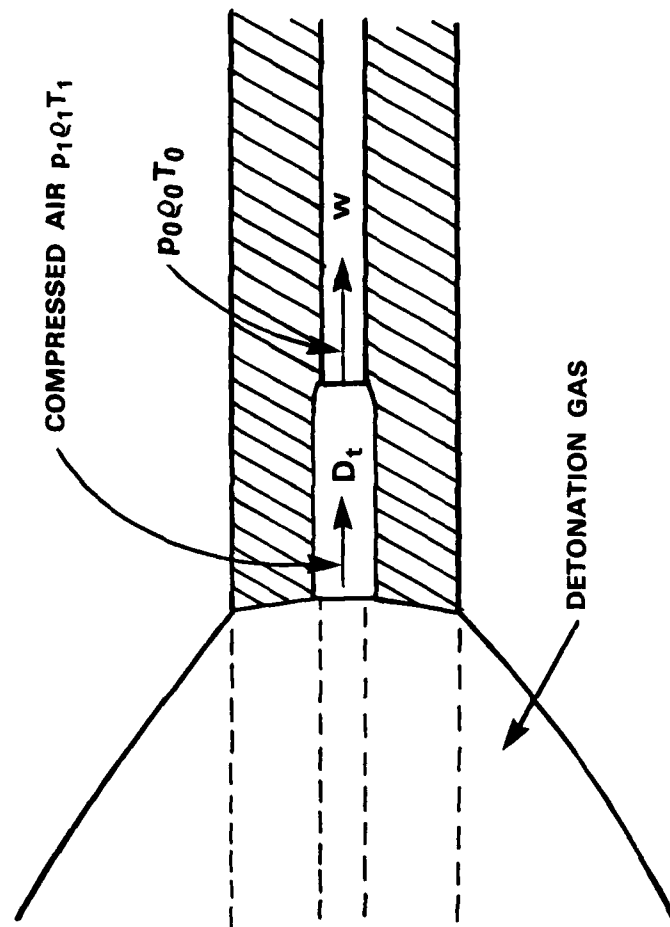


Figure 32
MODEL FOR CHANNEL EFFECT

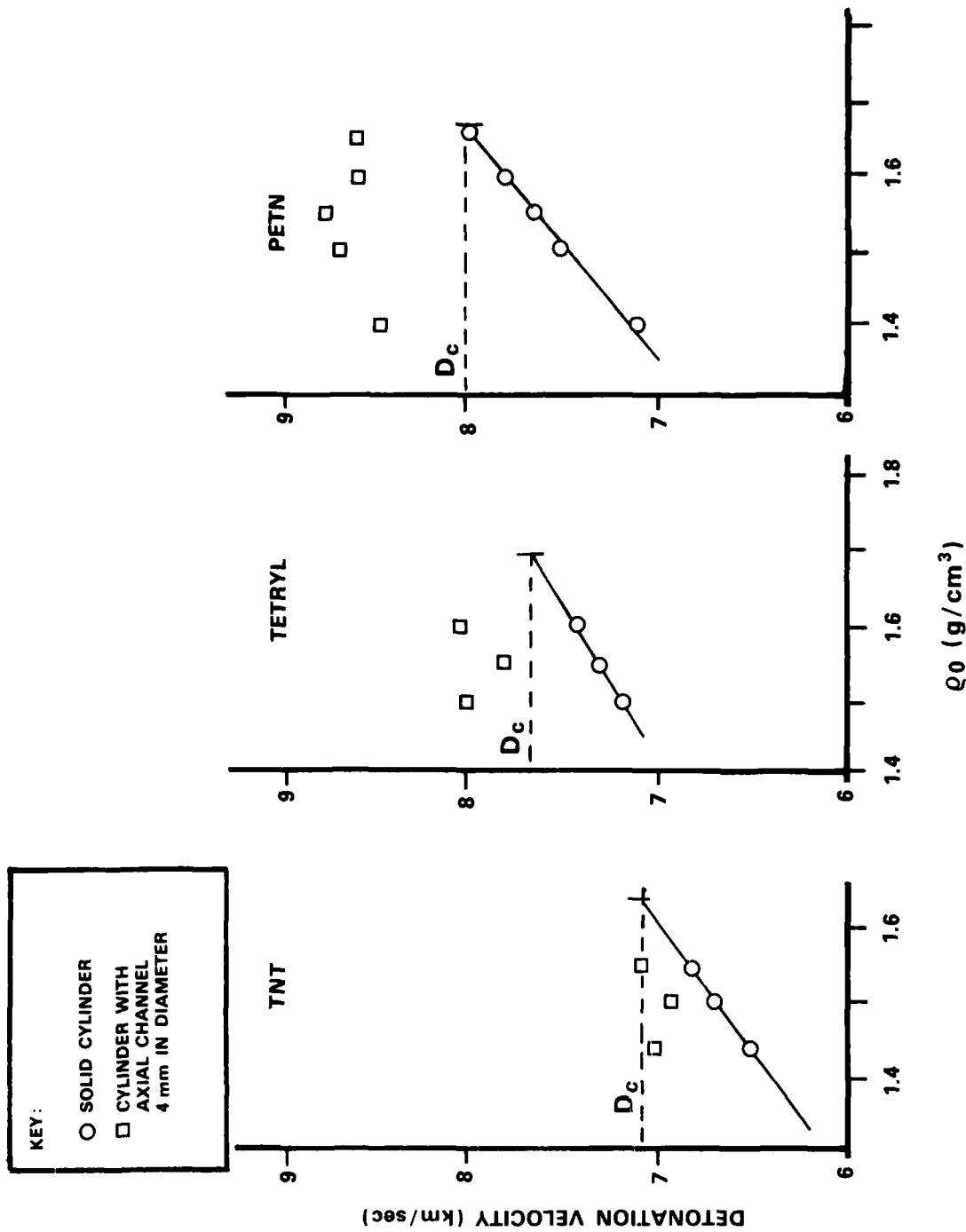
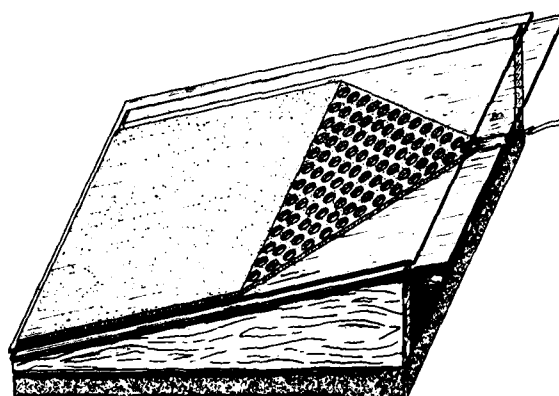
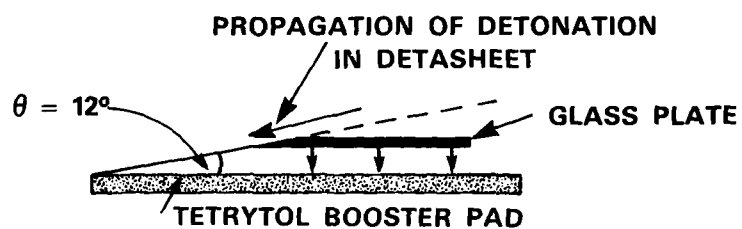


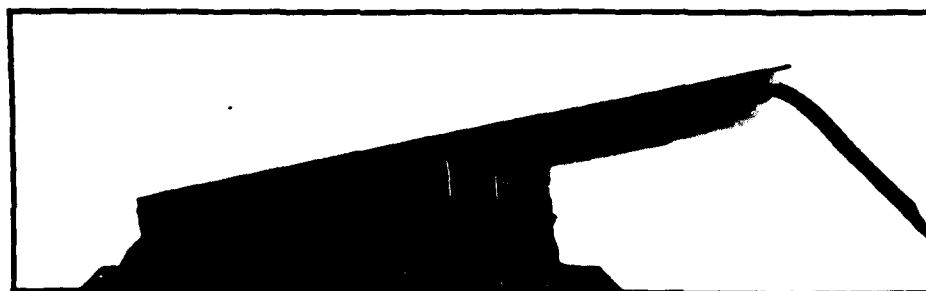
Figure 33
 DETONATION VELOCITIES IN CYLINDERS OF HIGH EXPLOSIVES
 21 mm IN DIAMETER AFTER AHRENS (1965)



(a) DEVICE BEFORE DETONATION



(b) SIDE VIEW OF DETONATING DEVICE



(c) PHOTOGRAPH OF DEVICE

Figure 34

MOUSETRAP — TYPE PLANE-WAVE GENERATOR

DOCUMENT CONTROL DATA - R & D

(Security classification of title, body of abstract and indexing annotation must be entered when the overall document is classified)

1 ORIGINATING ACTIVITY Defence Research Establishment Suffield		2a. DOCUMENT SECURITY CLASSIFICATION UNCLASSIFIED	
		2b. GROUP	
3 DOCUMENT TITLE THE EFFECT OF AIR GAPS ON THE PROPAGATION OF DETONATION IN CHARGES CONSISTING OF STACKED BLOCKS OF CAST TNT (U).			
4 DESCRIPTIVE NOTES (Type of report and inclusive dates) REPORT			
5 AUTHOR(S) (Last name, first name, middle initial) Gibb, A.W.			
6 DOCUMENT DATE December 1985		7a. TOTAL NO. OF PAGES 78	7b. NO. OF REFS 16
8a. PROJECT OR GRANT NO. 27C20		9a. ORIGINATOR'S DOCUMENT NUMBER(S) Suffield Report No. 385	
8b. CONTRACT NO.		9b. OTHER DOCUMENT NO.(S) (Any other numbers that may be assigned this document)	
10 DISTRIBUTION STATEMENT UNCLASSIFIED UNLIMITED			
11 SUPPLEMENTARY NOTES		12. SPONSORING ACTIVITY	
13 ABSTRACT A series of experiments was conducted to examine the influence on the uniformity of detonation propagation of air gaps between large blocks of slow-cooled cast TNT. Donor-receptor geometries examined were (i) two blocks with the detonation front parallel to the gap edge, and (ii) four blocks with one corner in common and the (planar) detonation front at an angle of 45° to the block edge. Air gaps from 3 mm to 25 mm were studied. The two-block configurations produced no distortion of the shape, but the measured detonation velocity in the donor blocks and the scatter in results in the receptor blocks were observed to be influenced by the orientation of the propagation velocity vector with respect to the long axis of the TNT crystals. The four-block configuration featured channelling of detonation gases ahead of the front in the air gaps, leading to an initially complex and distorted wave structure, as well as to a delay in reinitiation, in the vertically-opposite receptor block. The shape distortion and delay effects increased as the gap width was increased.			

KEY WORDS

1. Air Gap
2. Detonation
3. Propagation
4. Slow-Cooled;
5. Cast TNT
6. TNT Block
7. Donor-Receptor
8. Crystal Orientation
9. Channelling.

INSTRUCTIONS

1. **ORIGINATING ACTIVITY.** Enter the name and address of the organization issuing the document.
2. **DOCUMENT SECURITY CLASSIFICATION.** Enter the overall security classification of the document including special warning terms whenever applicable.
- 2b. **GROUP.** Enter security reclassification group number. The three groups are defined in Appendix 'M' of the DRB Security Regulations.
3. **DOCUMENT TITLE.** Enter the complete document title in all capital letters. Titles in all cases should be unclassified. If a sufficiently descriptive title cannot be selected without classification, show title classification with the usual one capital-letter abbreviation in parentheses immediately following the title.
4. **DESCRIPTIVE NOTES.** Enter the category of document, e.g. technical report, technical note or technical letter. If appropriate, enter the type of document, e.g. interim, progress, summary, annual or final. Give the inclusive dates when a specific reporting period is covered.
5. **AUTHOR(S).** Enter the name(s) of author(s) as shown on or in the document. Enter last name, first name, middle initial, if military, show rank. The name of the principal author is an absolute minimum requirement.
6. **DOCUMENT DATE.** Enter the date (month, year) of Establishment approval for publication of the document.
7. **TOTAL NUMBER OF PAGES.** The total page count should follow normal pagination procedures, i.e., enter the number of pages containing information.
- 7b. **NUMBER OF REFERENCES.** Enter the total number of references cited in the document.
- 8a. **PROJECT OR GRANT NUMBER.** If appropriate, enter the applicable research and development project or grant number under which the document was written.
- 8b. **CONTRACT NUMBER.** If appropriate, enter the applicable number under which the document was written.
- 9a. **ORIGINATOR'S DOCUMENT NUMBER(S).** Enter the official document number by which the document will be tracked and controlled by the originating activity. This number must be unique to this document.
- 9b. **OTHER DOCUMENT NUMBER(S).** If the document has been assigned any other document numbers (either by the originator or by the sponsor), also enter this number(s).
10. **DISTRIBUTION STATEMENT.** Enter any limitations on further dissemination of the document, other than those imposed by security classification, using standard statements such as:
 - (1) "Qualified requesters may obtain copies of this document from their defence documentation center."
 - (2) "Announcement and dissemination of this document is not authorized without prior approval from originating activity."
11. **SUPPLEMENTARY NOTES.** Use for additional explanatory notes.
12. **SPONSORING ACTIVITY.** Enter the name of the departmental project office or laboratory sponsoring the research and development. Include address.
13. **ABSTRACT.** Enter an abstract giving a brief and factual summary of the document, even though it may also appear elsewhere in the body of the document itself. It is highly desirable that the abstract of classified documents be unclassified. Each paragraph of the abstract shall end with an indication of the security classification of the information in the paragraph (unless the document itself is unclassified) represented as (TS), (S), (IC), (R), or (U).

The length of the abstract should be limited to 20 single-spaced standard typewritten lines, 7 1/2 inches long.
14. **KEY WORDS.** Key words are technically meaningful terms or short phrases that characterize a document and could be helpful in cataloging the document. Key words should be selected so that no security classification is required. Identifiers, such as equipment model designation, trade name, military project code name, geographic location, may be used as key words but will be followed by an indication of technical context.

END

FILMED

2-86

DTIC